



1
2 An updated synthesis of ocean total alkalinity and dissolved inorganic carbon measurements
3 from 1993 to 2023: the SNAPO-CO₂-v2 dataset

4
5 Nicolas Metzl¹, Jonathan Fin^{1,2,3}, Claire Lo Monaco¹, Claude Mignon¹, Samir Alliouane⁴, Bruno Bombled⁵,
6 Jacqueline Boutin¹, Yann Bozec⁶, Steeve Comeau⁴, Pascal Conan^{7,8}, Laurent Coppola^{4,8}, Pascale Cuet⁹, Eva
7 Ferreira⁵, Jean-Pierre Gattuso^{4,10}, Frédéric Gazeau⁴, Catherine Goyet¹¹, Emilie Grossteffan¹², Bruno Lansard⁵,
8 Dominique Lefèvre¹³, Nathalie Lefèvre¹, Coraline Leseurre¹⁴, Sébastien Petton¹⁵, Mireille Pujo-Pay⁸, Christophe
9 Rabouille⁵, Gilles Reverdin¹, Céline Ridame¹, Peggy Rimmelmaury¹², Jean-François Ternon¹⁶, Franck
10 Touratier¹¹, Aline Tribollet¹, Thibaut Wagener¹³, Cathy Wimart-Rousseau¹⁷.

11
12 ¹ Laboratoire LOCEAN/IPSL, Sorbonne Université-CNRS-IRD-MNHN, Paris, 75005, France

13 ² OSU Ecce Terra, Sorbonne Université-CNRS, Paris, 75005, France

14 ³ Now at Institut des Sciences de la Terre, Grenoble, 38058, France

15 ⁴ Sorbonne Université, CNRS, Laboratoire d'Océanographie de Villefranche, LOV, F-06230 Villefranche-sur-
16 Mer, France

17 ⁵ Laboratoire des Sciences du Climat et de l'Environnement, LSCE/IPSL, UMR 8212 CEA- CNRS-UVSQ,
18 Université Paris-Saclay, 91191 Gif-sur-Yvette, France

19 ⁶ Station Biologique de Roscoff, UMR 7144 – EDYCO-CHIMAR, Roscoff, France

20 ⁷ Sorbonne Université, CNRS, Laboratoire d'Océanographie Microbienne, LOMIC, F-66650 Banyuls-sur-Mer,
21 France

22 ⁸ Sorbonne Université, CNRS OSU STAMAR - UAR2017, 4 Place Jussieu, 75252, Paris cedex 05, France

23 ⁹ Laboratoire ENTROPIE and Laboratoire d'Excellence CORAIL, Université de La Réunion-IRD- CNRS-
24 IFREMER-Université de la Nouvelle-Calédonie, 97744, Saint-Denis, La Réunion, France

25 ¹⁰ Institute for Sustainable Development and International Relations, Sciences Po, 27 rue Saint Guillaume, F-
26 75007 Paris, France

27 ¹¹ Espace-Dev UMR 228 Université de Perpignan Via Domitia, IRD, UM, UA, UG, 66860, Perpignan, France

28 ¹² Institut Universitaire Européen de la Mer (OSU-IUEM), Univ Brest, CNRS-UAR3113, 29280, Plouzané,
29 France

30 ¹³ Aix Marseille Univ, Université de Toulon, CNRS, IRD, MIO, Marseille, France

31 ¹⁴ Flanders Marine Institute (VLIZ), 8400 Ostend, Belgium

32 ¹⁵ Ifremer, Univ Brest, CNRS, IRD, LEMAR, F-29840 Argenton, France

33 ¹⁶ MARBEC, Univ Montpellier, CNRS, Ifremer, IRD, Sète, France

34 ¹⁷ National Oceanography Centre Southampton, European Way, Southampton, SO14 3ZH, UK

35
36 *Correspondence to:* Nicolas Metzl (nicolas.metzl@locean.ipsl.fr)

37
38 **Abstract.** Total alkalinity (A_T) and dissolved inorganic carbon (C_T) in the oceans are important properties to
39 understand the ocean carbon cycle and its link with global change (ocean carbon sinks and sources, ocean
40 acidification) and ultimately find carbon based solutions or mitigation procedures (marine carbon removal). We
41 present an extended database (SNAPO-CO₂, Metzl et al, 2024d) with 24700 new additional data for the period
42 2002 to 2023. The full database now includes more than 67000 A_T and C_T observations along with basic
43 ancillary data (time and space location, depth, temperature and salinity) in various oceanic regions obtained since
44 1993 mainly in the frame of French research projects. This includes both surface and water columns data
45 acquired in open oceans, coastal zones, rivers and in the Mediterranean Sea and either from time-series or
46 punctual cruises. Most A_T and C_T data in this synthesis were measured from discrete samples using the same
47 closed-cell potentiometric titration calibrated with Certified Reference Material, with an overall accuracy of ± 4
48 $\mu\text{mol kg}^{-1}$ for both A_T and C_T . The same technique was used onboard for underway measurements during cruises



49 conducted in the Southern Indian and Southern Oceans. The A_T and C_T data from these cruises are also added in
50 this synthesis. The data are provided in one dataset for the global ocean (<https://doi.org/10.17882/102337>) that
51 offers a direct use for regional or global purposes, e.g. A_T /Salinity relationships, long-term C_T estimates,
52 constraint and validation of diagnostics C_T and A_T reconstructed fields or ocean carbon and coupled
53 climate/carbon models simulations, as well as data derived from Biogeochemical-Argo (BGC-Argo) floats.
54 These data can also be used to calculate pH, fugacity of CO_2 ($f\text{CO}_2$) and other carbon system properties to derive
55 ocean acidification rates or air-sea CO_2 fluxes.

56

57 **1 Introduction**

58

59 The ocean plays a major role in reducing the impact of climate change by absorbing more than 90% of
60 the excess heat in the climate system (Cheng et al., 2020, 2024; von Schuckmann et al, 2023; IPCC, 2022) and
61 about 25% of human released CO_2 (Friedlingstein et al., 2022, 2023). In the last decade, the oceans experienced
62 a rapid warming, the year 2023 being the hottest since 1955 (Cheng et al, 2024). In the atmosphere the CO_2
63 concentration continues its terrific progressive rising, reaching 419.3 ppm in 2023 (a rate of +2.83 ppm yr⁻¹, Lan
64 et al 2024). In August 2024, the global atmospheric CO_2 concentration was already above 420 ppm. In the next
65 decade the oceans will continue to capture heat and CO_2 , somehow limiting the climate change, but this oceanic
66 CO_2 uptake changes the chemistry of seawater reducing its buffering capacity (Revelle and Suess, 1957; Jiang et
67 al, 2023). This process known as ocean acidification has potential impacts on marine organisms (Fabry et al.,
68 2008; Doney et al., 2009, 2020; Gattuso et al., 2015). With atmospheric CO_2 concentrations, surface ocean
69 temperature and ocean heat content, sea-level, sea-ice and glaciers, the ocean acidification (decrease of pH) is
70 now recognized by the World Meteorological Organization as one of the 7 key properties for global climate
71 indicators (WMO, 2018). Ocean acidification is specifically referred in the SDG indicator 14.3.1 coordinated at
72 the Intergovernmental Oceanographic Commission (IOC) of UNESCO. Observing the carbonate system in the
73 open oceans, coastal zones and marginal seas and understanding how this system changes over time is thus
74 highly relevant not only to quantify the global ocean carbon budget, the anthropogenic CO_2 inventories or ocean
75 acidification rates, but also to understand and simulate the processes that govern the complex CO_2 cycle in the
76 ocean (e.g. Goyet et al, 2016, 2019) and to better predict the future evolution of climate and global changes
77 (Eyring et al., 2016; Kwiatkowski et al., 2020; Jiang et al., 2023). As the rate of change in ocean acidification
78 presents large temporal and regional variability, long-term observations are required. Weekly to monthly regular
79 resolution data are needed to better investigate the long-term change of the carbonate system in regions subject
80 to extreme events (e.g. tropical cyclones, marine heat or cold waves, rapid freshening, convection, dust events,
81 river discharges, etc...). In this context it is recommended to progress in data synthesis of the ocean carbon
82 observations that would offer new high quality products for the community (e.g. for GOA-ON, www.goa-on.org,
83 IOC/SDG 14.1.3, <https://oa.iode.org/>, Tilbrook et al., 2019).

84 In this work, following the first SNAPO- CO_2 synthesis product (Metzl et al, 2024a), we present a new
85 synthesis of more than 67000 A_T and C_T data, measured either on shore or onboard Research Vessels obtained
86 over the 1993-2023 period during various cruises or at time-series stations mainly supported by French projects.
87 Hereafter this new dataset will be cited as SNAPO- CO_2 -v2. The methods, data assemblage and quality control



88 were presented in version V1. Here, we describe the new data added and discuss some potential uses of this
89 dataset.

90

91 2 Data collections

92

93 The time series projects and research cruises from which new data were collated are listed in Table 1
94 with information and references in the Supplementary file (Tables S1, S3 and S4). The sampling locations of
95 new data are displayed in Figure 1 (the location for all data presented in Figure S1). Sampling was performed
96 either from CTD-Rosette casts (Niskin bottles) or from the ship's seawater supply (intake at about 5m depth
97 depending on the ship and swell). Samples collected in 500 mL borosilicate glass bottles were poisoned with 100
98 to 300 μL of HgCl_2 depending on the cruises, closed with greased stoppers (Apiezon®) and held tight using
99 elastic band following the SOP protocol (DOE, 1994; Dickson et al., 2007). Some samples were also collected in
100 500 mL bottles closed with screw caps. After completion of each cruise, most of discrete samples were returned
101 back to the LOCEAN laboratory (Paris, France) and stored in a dark room at 4 °C before analysis generally
102 within 2-3 months after sampling (sometimes within a week). In this version we added data from samples that
103 were also returned to University of Perpignan or to University of La Réunion. In addition to discrete samples
104 analyzed for various projects conducted mainly in the North Atlantic, Tropical Atlantic, Mediterranean Sea and
105 coastal regions (Table 1), we complemented this second synthesis with A_T and C_T surface observations obtained
106 in the Indian and Southern oceans during the OISO cruises in 2019-2021 (Leseurre et al., 2022; Metzl et al,
107 2022; data also available at NCEI/OCADS: www.nodc.noaa.gov/ocads/oceans/VOS_Program/OISO.html) and
108 MINERVE cruises in 2002-2018 (Laika et al, 2009; Brandon et al, 2022). The A_T and C_T measurements from the
109 MINERVE cruises were performed either onboard R/V Astrolabe or back in the laboratories (at LOCEAN
110 laboratory and at University of Perpignan).

111

112

113

114

115

116

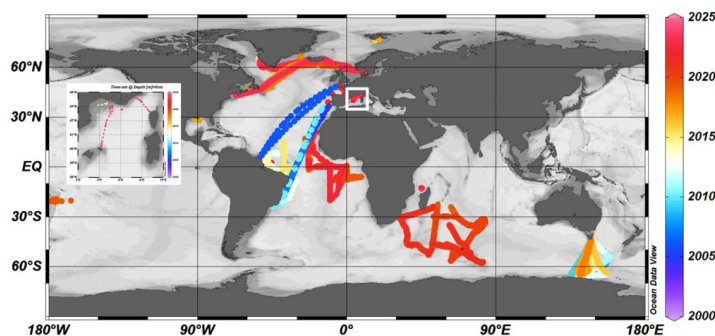
117

118

119

120

121



122 **Figure 1:** Locations of new A_T and C_T data (2005-2023) in the Global Ocean and the Western Mediterranean Sea
123 (white box, insert) in the SNAPO-CO2-v2 dataset. Color code is for Year. Figure produced with ODV (Schlitzer,
124 2018).

125



126 **Table 1:** List of cruises added in the SNAPO-CO₂-v2 dataset. This is organized by region from North to South
 127 and the Mediterranean Sea. See Tables S1, S2, S3 and S4 in the Supplementary Material for a list of laboratories,
 128 of CRMs used, for DOI and for references of cruises. Nb = the number of data for each cruise or time-series. *
 129 indicates the measurements at sea (surface underway).

Cruise/Project	Start	End	Region	Sampling	Nb	
135	STEP	2016	2017	Arctic	Water Column	33
136	SURATLANT AX1	2017	2023	North Atlantic	Surface	255
137	SURATLANT AX2	2018	2023	North Atlantic	Surface	224
138	VOS	2005	2010	Atlantic	Surface	192
139	MISSRHODIA-1	2017	2017	Gulf Mexico	Water Column	8
140	ACIDHYPO	2022	2022	Gulf Mexico	Water Column	10
141	CAMFIN-WATL	2010	2015	Trop Atlantic	Surface	192
142	PIRATA-BR	2009	2015	Trop Atlantic	Surface	194
143	BIOAMAZON	2013	2014	Trop Atlantic	Surface	62
144	AMAZOMIX	2021	2021	Trop Atlantic	Water Column	180
145	PIRATA-FR	2019	2019	Trop Atlantic	Surface	93
146	PIRATA-FR	2020	2020	Trop Atlantic	Surface, Water Column	58
147	PIRATA-FR	2021	2021	Trop Atlantic	Surface, Water Column	79
148	PIRATA-FR	2022	2022	Trop Atlantic	Surface, Water Column	118
149	CO2ARVOR	2009	2010	Atlantic, Coastal	Surface, Water Column	621
150	SOMLIT-Roscoff	2020	2022	Coastal North Atl	Surface and 60m	207
151	SOMLIT-Brest	2020	2022	Coastal North Atl	Surface	251
152	TONGA	2019	2019	Trop Pacific	Water Column	226
153	CARBODISS	2018	2019	Indian Mayotte	Surface	85
154	OISO *	2019	2021	South Indian	Surface	5258
155	MINERVE	2004	2018	Southern Ocean	Surface	1077
156	MINERVE *	2002	2013	Southern Ocean	Surface	11258
157	COCORICO2	2017	2022	Coastal	Surface	589
158	SOMLIT-PointB	2019	2023	MedSea Coastal	Surface and 50m	716
159	SOLEMIO	2018	2022	MedSea Coastal	Water Column	271
160	ANTARES	2017	2023	MedSea	Water Column	506
161	MOLA	2018	2023	MedSea Coastal	Water Column	193
162	DYFAMED	2018	2023	MedSea	Water Column	514
163	MESURHO-BENT	2010	2011	MedSea Coastal	Surface and sub-surface	25
164	ACCESS-01	2012	2012	MedSea Coastal	Water Column	16
165	CARBO-DELTA-2	2013	2013	MedSea Coastal	Water Column	14
166	DICASE	2014	2014	MedSea Coastal	Water Column	22
167	MISSRHODIA-2	2018	2018	MedSea Coastal	Surface and sub-surface	13
168	DELTARHONE1	2022	2022	MedSea Coastal	Water Column	9
169	MOOSE-GE	2021	2021	MedSea	Water Column	451
170	MOOSE-GE	2022	2022	MedSea	Water Column	447
171	MOOSE-GE	2023	2023	MedSea	Water Column	475

174 **3 Method, accuracy, repeatability and quality control**

176 **3.1 Method and accuracy**

178 Since 2003, the discrete samples returned back at SNAPO-CO₂ Service facilities (LOCEAN, Paris),
 179 were analyzed simultaneously for A_T and C_T by potentiometric titration using a closed cell (Edmond, 1970;
 180 Goyet et al., 1991). The same technique was used at sea for surface water underway measurements during OISO
 181 and MINERVE cruises (indicated by * in Table 1). In the late 1980s the so-called “JGOFS-IOC Advisory Panel
 182 on Ocean CO₂” recommended the need for standard analysis protocols and for developing Certified Reference
 183 Materials (CRMs) for inorganic carbon measurements (Poisson et al., 1990; UNESCO, 1990, 1991). The CRMs



184 were provided to international laboratories by Pr. A. Dickson (Scripps Institution of Oceanography, San Diego,
185 USA), starting in 1990 for C_T and 1996 for A_T , respectively. These CRMs were thus always available to us and
186 used to calibrate the measurements (CRM Batch numbers used for each cruise are listed in the Supplementary
187 file, Table S2). The CRMs accuracy, as indicated in the certificate for each Batch, is around $\pm 0.5 \mu\text{mol kg}^{-1}$ for
188 both A_T and C_T (www.nodc.noaa.gov/ocads/oceans/Dickson_CRM/batches.html). The concentrations of CRMs
189 we used vary between 2193 and 2426 $\mu\text{mol kg}^{-1}$ for A_T and between 1968 and 2115 $\mu\text{mol kg}^{-1}$ for C_T
190 corresponding to the range of concentrations observed in open ocean water. In the Mediterranean Sea the
191 concentrations are higher ($A_T > 2600 \mu\text{mol kg}^{-1}$ and $C_T > 2300 \mu\text{mol kg}^{-1}$) and in the coastal zones or near the
192 Amazon River plume the concentrations were often lower than the CRMs ($A_T < 1500 \mu\text{mol kg}^{-1}$ and $C_T < 1000$
193 $\mu\text{mol kg}^{-1}$). Results of analyses performed on 1242 CRM bottles (different Batches) in 2013-2024 are presented
194 in Figure 2. The standard-deviations (Std) of the differences of measurements were on average $\pm 2.69 \mu\text{mol kg}^{-1}$
195 for A_T and $\pm 2.88 \mu\text{mol kg}^{-1}$ for C_T . For unknown reasons, the differences were occasionally up to $10\text{-}15 \mu\text{mol kg}^{-1}$
196 (1.2% of the data, Figure S2). These few CRM measurements were discarded for the data processing. We did
197 not detect any specific signal for CRM analyses (e.g., larger uncertainty depending on the Batch number or
198 temporal drifts during analyses, Figure 2) but for some cruises the accuracy based on CRMs could be better than
199 $3 \mu\text{mol kg}^{-1}$ (e.g. $< 3 \mu\text{mol kg}^{-1}$ for AMAZOMIX cruise using 6 Batches #197 and for MOOSE-GE 2022 using
200 19 Batches #204, or $< 1.5 \mu\text{mol kg}^{-1}$ for SOMLIT-Point-B in 2022 using 6 Batches #204).

201
202
203
204
205
206
207
208
209
210
211
212
213
214
215
216
217
218
219
220
221
222
223
224
225
226

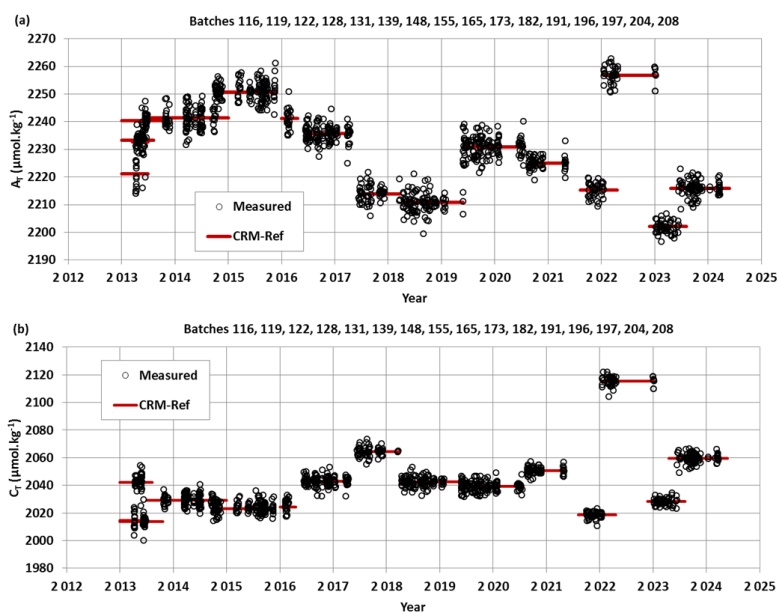


Figure 2: A_T (a) and C_T (b) analyses for different CRM Batches measured in 2013-2024. For these 1242 analyses the mean and standard-deviations of the differences with the CRM reference were $-0.11 (\pm 2.69) \mu\text{mol kg}^{-1}$ for A_T and $0.01 (\pm 2.88) \mu\text{mol kg}^{-1}$ for C_T .



227 3.2 Repeatability

228

229 For some projects, duplicates have been regularly sampled (SOMLIT-Point-B, SOMLIT-Brest) or
230 replicate bottles sampled at selected depths at fixed stations during the cruises (e.g. STEP, CARBODISS). In the
231 first synthesis of the SNAPO-CO2 dataset we showed the results from several time-series (SOMLIT-Point-B,
232 SOMLIT-Brest and BOUSSOLE/DYFAMED). Here we present the results for the new data obtained at
233 SOMLIT-Point-B in the coastal Mediterranean Sea and SOMLIT-Brest in the Bay of Brest (Figure 3). Results of
234 A_T and C_T repeatability are synthesized in Table 2. For the OISO cruises conducted in 2019, 2020 and 2021 the
235 repeatability was evaluated from duplicate analyses (within 20 minutes time) of continuous sea surface
236 underway sampling at the same location (when the ship was stopped). Similarly to what was found for the CRM
237 measurements (Figure S2), differences in duplicates are occasionally higher than $10\text{--}15\ \mu\text{mol kg}^{-1}$ (Figure 3) but
238 most of the duplicates for all projects are within 0 to $3\ \mu\text{mol kg}^{-1}$. Compared to previous results (Kapsenberg et
239 al. 2017; Metz1 et al, 2024a), there are larger differences between duplicates at SOMLIT-B in 2019–2023 (up to
240 $30\ \mu\text{mol kg}^{-1}$, Figure 3) leading to relatively large Std around 5 and $6\ \mu\text{mol kg}^{-1}$ for both A_T and C_T (Table 2).
241 The same was observed for duplicates at SOMLIT-Brest (Table 2). We do have not yet a clear explanation for
242 this large Std although larger variability was observed in recent years, and the measurements were performed
243 later after the sampling (e.g. more than 6 months for some samples during and after the COVID period). We will
244 see that given the temporal variability of the properties this does not lead to suspicious interpretation for the
245 seasonality or the trend analyses of these time-series.

246

247

248

249

250

251

252

253

254

255

256

257

258

259

260

261

262

263

264

265

266

267

268

269

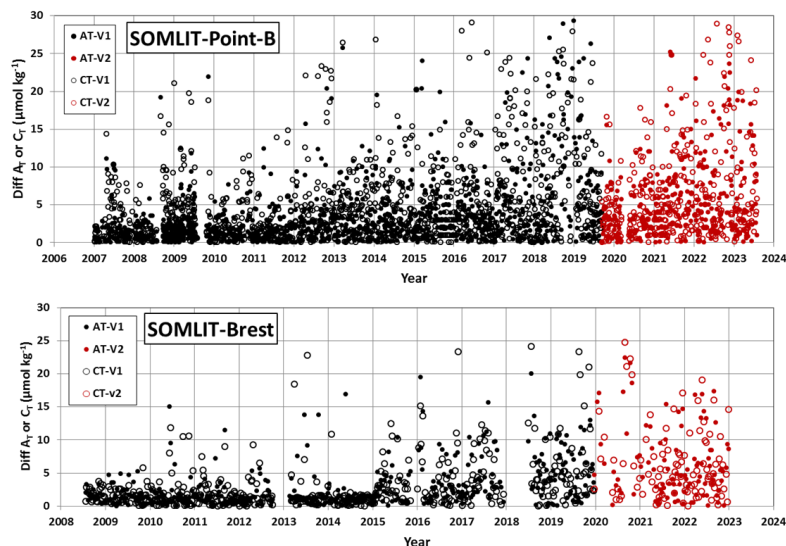


Figure 3: Results of duplicate A_T and C_T analyses from the time-series SOMLIT-Point-B in the coastal
Mediterranean Sea and SOMLIT-Brest in the coastal Brittany for the data in the SNAPO-CO2-v1 dataset (black)
and new data added in SNAPO-CO2-v2 (red). The plots show differences in duplicates for both A_T (filled
circles) and C_T (open circles). Standard-deviations of these duplicates are listed in Table 2.



270 **Table 2:** Repeatability of A_T and C_T analyses for cruises with duplicate analysis. The results are expressed as the
271 standard-deviations (Std) of the analysis of replicated samples. Nb = the number of replicates for each Time-
272 series or Cruise. For the OISO cruises the mean repeatability was obtained from measurements at the same
273 location (when the ship stopped).

Cruise	Period	Nb	Std A_T $\mu\text{mol kg}^{-1}$	Std C_T $\mu\text{mol kg}^{-1}$	Reference
STEP	2017	3	0.7	2.8	Unpublished
CARBODISS	2018	10	6.72	5.71	Unpublished
SOMLIT-Point-B	2007-2019	1130	4.5	5.1	SNAPO-CO2-v1
SOMLIT-Point-B	2019-2023	321	5.2	6.2	SNAPO-CO2-v2
SOMLIT-Brest	2008-2018	404	3.1	3.4	SNAPO-CO2-v1
SOMLIT-Brest	2019-2022	142	6.0	6.1	SNAPO-CO2-v2
OISO 29	2019	46	1.8	1.8	Leseurre et al (2022), (b)
OISO 30	2020	67	1.5	2.0	Metzl et al. (2022), (b)
OISO 31	2021	343	2.6	3.3	Metzl et al (2024c), (b)

293 (a) See Figure 3 for the results of regular duplicates for time-series SOMLIT-Point-B, SOMLIT-Brest.

294 (b) Metadata and data available at www.nodc.noaa.gov/ocads/oceans/VOS_Program/OISO.html

296 3.3 Assigned flags for quality control

297
298 Identifying each data with an appropriate flag is very convenient for selecting the data (good,
299 questionable or bad). Here we used 4 flags for each property (flags 2 = good, 3= questionable, 4=bad, and 9= no
300 data) following the WOCE program and used in other data products such as SOCAT (Bakker et al., 2016) or
301 GLODAP (Olsen et al., 2016; Lauvset et al., 2024). During the data-processing, we first assigned a flag for each
302 A_T and C_T data based on the standard error in the calculation of A_T and C_T concentrations (non-linear regression,
303 Dickson et al. 2007). By default, if the standard deviation on the regression is $> 1 \mu\text{mol kg}^{-1}$, we assigned a flag 3
304 (questionable) although the data could be acceptable and then used for interpretations. Flag 3 was also assigned
305 when salinity was doubtful or when differences of duplicates were large (e.g. $\pm 20 \mu\text{mol kg}^{-1}$). Flags 4 (bad or
306 certainly bad) were assigned when clear anomalies were detected for unknown reasons (e.g. a sample probably
307 not fixed with HgCl_2 or analysis performed late during the COVID issue). A secondary quality control was
308 performed by the PIs of each project based on data inspection, duplicates, A_T /Salinity relationship, or the mean
309 observations in deep layers where large variability in A_T and C_T is unlikely to occur from year to year.

310 An example for quality flag is presented for all data from the MINERVE cruises conducted in 2002-
311 2018 in the Southern Ocean where clear outliers have been identified (Figure S3). For the MINERVE cruises in
312 2002-2018 and a total of 12335 A_T and C_T analyses, 24 were identified as bad (flag 4), 978 for A_T and 971 for C_T
313 listed as questionable (flag 3), and all others are considered as good data (flag 2, i.e. about 92%). For the
314 MOOSE-GE cruises in 2021, 2022 and 2023 (new data in SNAPO-CO2-v2) and a total of 1373 A_T and C_T
315 analyses, 2 were identified flagged as bad (flag 4), 38 for A_T and 33 for C_T listed as questionable (flag 3) all
316 others were considered as good data (flag 2, i.e. 97%). This is better than the statistics we evaluated for the
317 SNAPO-CO2-v1 dataset (90% flag 2 for MOOSE-GE in 2010-2019). A similar control was performed for each
318 project.



319 **3.4 Inter-comparisons**

320

321 Inter-comparisons of measurements performed for different cruises or with different techniques help
322 evaluate the quality of the data and detect potential biases when merging the data in the same region obtained by
323 different laboratories at different periods. This is especially important to interpret long-term trends of A_T and C_T
324 as well as for pCO_2 and pH calculated with A_T C_T pairs. The synthesis of various cruises in the same region and
325 periods also offers verification and secondary control of the data.

326

327 **3.4.1 Comparisons in deep layers**

328

329 Comparisons of data in the deep layers from different cruises are useful for secondary quality control as
330 one expects low natural variability or anthropogenic signals from season to season and over a few years. Several
331 cruises were conducted in the Mediterranean Sea in 2017-2023 (MOOSE-GE, ANTARES and DYFAMED). The
332 mean values of C_T and A_T in the deep layers ($> 1800m$) for each cruise confirmed the coherence of the data
333 (Table 4). The C_T and A_T concentrations are also in the range of the mean values evaluated for cruises conducted
334 in 2014 in the Mediterranean Sea (results listed in the SNAPO-CO2-v1 synthesis, Metzl et al, 2024a). In the
335 western tropical Pacific we also observed coherent properties for the TONGA and OUTPACE cruises (Wagener
336 et al, 2018) for data selected at 1800-2300m layer corresponding to the C_T maximum layer in the Pacific Deep
337 Water (PDW). On the other hand in the western tropical Atlantic near the Amazon River plume where the spatial
338 variability of the properties is large at the surface (Ternon et al, 2000; Mu et al, 2021; Olivier et al, 2022) the
339 comparison in the water column is less clear (Figure S4). Nevertheless for the AMAZOMIX and the TARA-
340 Microbiome cruises, both conducted in September 2021, the results at close stations (around $5^{\circ}N/50^{\circ}W$) suggest
341 very similar concentrations at 1000m (Table 4). The comparisons in deep waters enabled to merge the different
342 datasets for interpretations of the temporal trends and processes driving the CO_2 cycle in these regions (e. g.
343 Ulses et al., 2023 and Wimart-Rousseau et al., 2023 for the Mediterranean Sea)

344

345 **3.4.2 Comparing on board and on shore results**

346

347 In surface waters where the variability is high inter-comparison is not relevant for secondary quality
348 control. However, during the MINERVE cruises, discrete samples were occasionally performed along with sea
349 surface underway measurements. Thus, we can compare A_T and C_T measured in the laboratory with those
350 measured onboard as described by Laika et al. (2009) for the MINERVE cruises in 2005-2006. It should be
351 noticed that the discrete samples were measured after a long trip (shipping boxes from Hobart, Tasmania to
352 Paris, France) and thus generally analyzed at least 3 months after the cruises (cruises conducted in October to
353 February, analyses performed in May-June). Given all the uncertainties associated to the sampling, samples
354 storage and transport, analyses and CRMs, the mean differences between discrete and underway data are still
355 reasonable (Std ranging between 4 and $12 \mu mol kg^{-1}$, Table 5). For unknown reasons the mean difference was
356 high for a cruise in 2008-2009 (Std $> 10 \mu mol kg^{-1}$, the “weather goal”, Newton et al., 2015). With this in mind,
357 we believe the MINERVE data (both underway and discrete data) are useful to interpret the change of properties
358 in this region at seasonal or decadal scales (Laika et al., 2009; Brandon et al., 2022).

359



360 **Table 4:** Mean observations in the deep layers (> 1800m) of the Ligurian Sea (Western Mediterranean Sea for
 361 different cruises conducted in 2017-2023), of the Tropical Pacific (around 2000m for cruises in 2017 and 2019),
 362 and of the Tropical Atlantic (around 1000m for cruises in 2021). $N-A_T$ and $N-C_T$ are A_T and C_T normalized at
 363 salinity ($S = 38$ in the Ligurian Sea; $S = 35$ for the Pacific and the Atlantic Oceans). Nb = number of data (with
 364 flag 2). Standard deviations are in brackets.
 365

Cruise	Period	Nb	Pot. Temp (°C)	Salinity	$N-A_T$ ($\mu\text{mol kg}^{-1}$)	$N-C_T$ ($\mu\text{mol kg}^{-1}$)
Ligurian Sea (> 1800m)						
All Cruises	2017-2023	227	12.923 (0.052)	38.484 (0.003)	2558.3 (10.5)	2300.0 (10.7)
DYFAMED	2017-2022	74	12.913 (0.006)	38.485 (0.002)	2555.1 (11.8)	2297.3 (12.4)
ANTARES	2017-2023	62	12.944 (0.096)	38.485 (0.005)	2559.8 (9.0)	2302.2 (8.9)
MOOSE-GE	2017-2023	91	12.917 (0.005)	38.484 (0.003)	2559.8 (9.8)	2300.7 (10.0)
Tropical Pacific (layer 1800-2300m)						
OUTPACE	2017	15	2.124 (0.055)	34.633 (0.006)	2414.1 (8.0)	2318.8 (5.8)
TONGA	2019	7	2.196 (0.197)	34.619 (0.016)	2408.9 (9.1)	2327.2 (7.5)
Western Tropical Atlantic (1000m)						
AMAZOMIX	2021	14	4.770 (0.105)	34.711 (0.041)	2315.6 (20.2)	2220.8 (17.1)
TARA-MICRO	2021	1	4.852	34.717	2312.9	2231.1

403 **Table 5:** Comparison of A_T and C_T analysed on-board and at SNAPO-CO2 facilities for the MINERVE project.
 404 The results are expressed as the standard deviations (Std) of the differences for each cruise. Nb = the number of
 405 co-located samples.
 406

Period	Nb	Std A_T $\mu\text{mol kg}^{-1}$	Std C_T $\mu\text{mol kg}^{-1}$
2004-2005	109	12.85	4.99
2005-2006	45	4.20	6.77
2007-2008	17	10.15	10.62
2008-2009	26	15.80	12.02
2009-2010	22	4.04	5.78
2010-2011	33	9.36	6.83
2012-2013	29	5.43	9.73



422 3.4.3 Comparison based on different techniques

423

424

425

426

427

428

429

430

431

432

433

434

435

436

437

438

439

440

441

442

443

444

445

446

447

448

449

450

451

452

453

454

455

456

457

458

459

460

461

462

463

464

465

466

Another example of comparison is presented for samples obtained in the lagoon of Mayotte Island in the western Indian Ocean and measured using different techniques. In the frame of the CARBODISS project seawater was sampled in 2018-2023 at several coral reef sites within the north-eastern part of the lagoon and measured either at LOCEAN laboratory or at La Réunion University. To remove coral sand particles the water samples were immediately filtered through Whatman GF/F filters and poisoned with mercuric chloride, following Dickson et al. (2007). In 2021, 2022 and 2023, A_T was measured at La Réunion University using an automated potentiometric titration (905 Titrando Metrohm titrator with combined pH electrode 6.0253.00) and calculated from the second inflection point of the titration curve. The HCl concentration was checked each day of measurements using a CRM provided by A. Dickson, Scripps Institution of Oceanography. The A_T precision based on triplicate was estimated $\pm 2 \mu\text{mol kg}^{-1}$ (Lagoutte et al., 2023). In the studied coral reef sites A_T concentrations ranged between 2250 and 2350 $\mu\text{mol kg}^{-1}$ but with occasional higher concentrations up to 2450-2500 $\mu\text{mol kg}^{-1}$. Such high A_T has been observed in other coral reefs ecosystems (Cyronak et al., 2013 at Cook Island; Palacio-Castro et al., 2023 at Middle Keys, Florida). The data obtained in the lagoon of Mayotte on different coral reefs could be compared with underway observations obtained offshore of Mayotte Island (OISO-11 cruises in 2004 and CLIM-EPARSEES cruise in 2019, data available in the SNAPO-CO2-v1 dataset). In the open ocean the A_T concentrations ranged between 2250 and 2330 $\mu\text{mol kg}^{-1}$, close to the results obtained at Mayotte reefs except for samples in November 2021 that were all collected at Cratère station (12.84°S-45.39°E) (Figure 4). At this location there was a large diurnal variation in November 2021 with A_T increasing from 2322 to 2508 $\mu\text{mol kg}^{-1}$ (Figure S5). This is because in 2021 the samples were taken at low tide recording a volcanic signal at this site allowing recording for the first time the volcanic signal in this location (CO_2 resurgences). In 2018 and 2019 such high A_T were not measured (Figure S5) as samples were taken at high tides allowing a certain dilution of volcanic CO_2 emissions in the water column. Although the samples were measured with different techniques the range of A_T is coherent for both datasets (Figure 4). Therefore we added the A_T data measured at La Réunion University in 2021-2023 to complete the synthesis for this location (Mayotte Island).

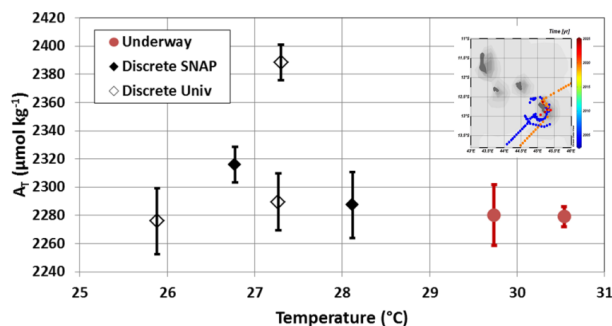


Figure 4: Total alkalinity (A_T) versus temperature for samples measured around Mayotte and in the coral reef (insert map). Underway A_T was measured onboard in 2004 and 2019 (red circles) whereas discrete samples at different reef sites within the lagoon of Mayotte in 2018, 2019, 2021, 2022 and 2023 were measured at LOCEAN (black diamonds) or at La Réunion University (open diamonds). The figure presents the data averaged for each cruise in this region.



467 3.4.4 Summary of quality control data

468

469 The total number of data in the SNAPO-CO₂-v2 dataset for the Global Ocean is gathered in Table 6
470 with corresponding flags for each property. Overall, the synthesis includes more than 91% of good data for both
471 A_T and C_T . About 6% are questionable and 3% are likely bad. Overall, we believe that all data (with flag 2) in
472 this synthesis have an accuracy better than 4 $\mu\text{mol kg}^{-1}$ for both A_T and C_T , the same as for quality-controlled
473 data in GLODAP (Lauvset et al., 2024). The uncertainty ranges between the “Climate goal” (2 $\mu\text{mol kg}^{-1}$) and
474 the “Weather Goal” (10 $\mu\text{mol kg}^{-1}$) for ocean acidification studies (Newton et al., 2015; Tilbrook et al., 2019).
475 This accuracy is also relevant to validate or constraint data-based methods that reconstruct A_T and C_T fields with
476 an error of around 10-15 $\mu\text{mol kg}^{-1}$ for both properties (Bittig et al., 2018; Broullón et al., 2019, 2020; Fourier et
477 al., 2020; Gregor and Gruber, 2021; Chau et al., 2024a).

478

479

480 **Table 6:** Number of Temperature, Salinity, A_T and C_T data in the SNAPO-CO₂-v2 synthesis identified for flags
481 2 (good), 3 (questionable), 4 (bad), 9 (no data). Last column is the percentage of flag 2 (Good).

482

483

Property	Flag 2	Flag 3	Flag 4	Flag 9	% flag 2
Temperature	68253	418	0	653	99.4
Salinity	68706	482	5	131	99.3
A_T	61249	3910	2077	2088	91.1
C_T	61869	3865	2057	1533	91.3

491

492

493 4 Global A_T and C_T distribution based on the SNAPO-CO₂-v2 dataset

494

495 The surface distribution in the global ocean based on the SNAPO-CO₂ dataset is presented in Figure 5
496 for A_T and C_T . The A_T /Salinity and A_T / C_T relationships are clearly identified and structured at regional scale
497 (Figure 6). In the open ocean, high A_T concentrations (> 2400 $\mu\text{mol kg}^{-1}$) are identified in the Atlantic subtropics
498 (bands 35°N-15°N and 25°S-3°S) (Jiang et al., 2014; Takahashi et al., 2014). The lowest A_T and C_T
499 concentrations (< 600 $\mu\text{mol kg}^{-1}$) are observed in the western tropical Atlantic in the Amazon River plume near
500 the mouth (Lefèvre et al., 2017b). For C_T the concentrations are high (> 2150 $\mu\text{mol kg}^{-1}$) in the Southern Ocean
501 south of the polar front, associated with the deep mixing in winter and the upwelling of deep water (Metzl et al.,
502 2006; Pardo et al., 2017). The highest C_T concentrations (up to 2180-2270 $\mu\text{mol kg}^{-1}$) are observed in the high
503 latitudes of the Southern Ocean near the Adélie coastal zone (MINERVE and ACE cruises), around the
504 Kerguelen plateau (OISO-31 cruise) and close to the Antarctic Peninsula (TARA-Microbiome cruise). In the
505 North Atlantic the new data from SURATLANT cruises in 2018-2023 confirm the high C_T concentrations (>
506 2150 $\mu\text{mol kg}^{-1}$) observed in the Sub-polar gyre since 2016 due in part to the accumulation of anthropogenic CO₂
507 (Leseurre et al., 2020). Low C_T concentration (< 2000 $\mu\text{mol kg}^{-1}$) are found in the tropics (10°N-30°S) with
508 lower values (< 1950 $\mu\text{mol kg}^{-1}$) in the equatorial Atlantic band 10°N-Eq (e.g. Koffi et al., 2010; Lefèvre et al.,
509 2021). In the Amazon shelf sector C_T can reach even lower concentration (< 1700 $\mu\text{mol kg}^{-1}$, AMAZOMIX
510 cruise).



511
512
513
514
515
516
517
518
519
520
521
522
523
524
525
526
527
528
529
530
531
532
533
534
535
536
537
538
539
540
541
542
543
544
545
546
547
548
549
550
551
552
553
554
555
556
557
558
559
560
561
562
563
564

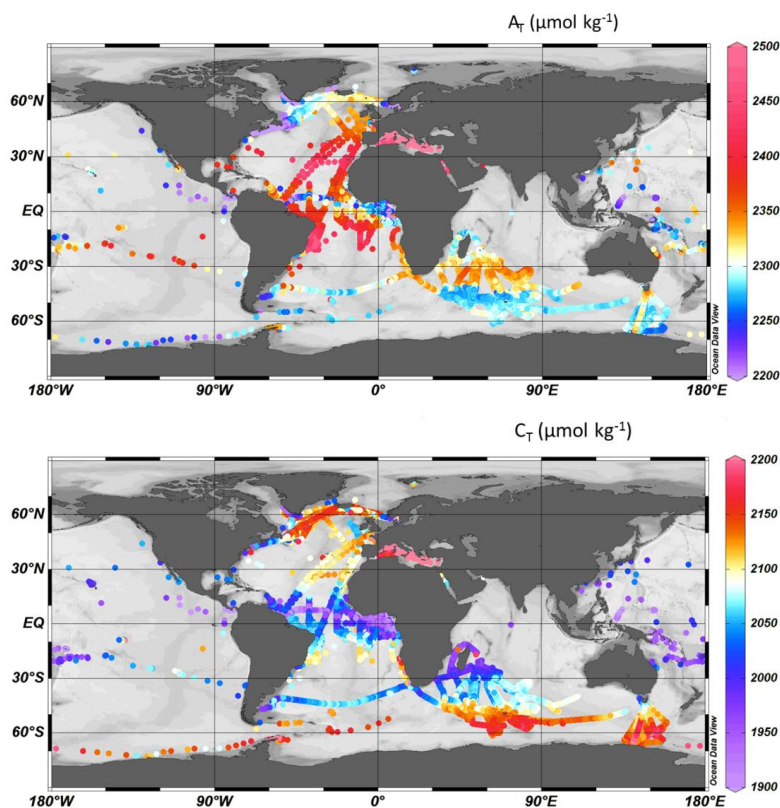


Figure 5: Distribution of A_T (top) and C_T (bottom) concentrations ($\mu\text{mol.kg}^{-1}$) in surface waters (0-10m) in the SNAPO-CO2-v2 dataset. Only data with flag 2 are presented in these figures. Figures produced with ODV (Schlitzer, 2018).

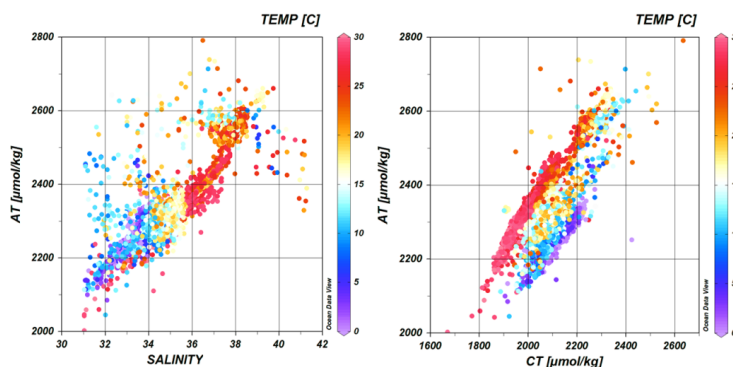


Figure 6: Relationships between A_T and Salinity (left panel) and A_T versus C_T (right panel) for samples in surface waters (0-10m and Salinity > 31). Only data with flag 2 are presented (nb = 48749). The color scales correspond to the temperature. The data not aligned correspond to coastal zones (e.g. COCORICO2 stations). Figures produced with ODV (Schlitzer, 2018).



565 5 Regional A_T and C_T distributions and trends based on the SNAPO-CO2 dataset

566

567 5.1 The Mediterranean Sea

568

569 Compared to the open ocean, A_T concentrations are much higher in the Mediterranean Sea (Copin-
570 Montégut, 1993; Schneider et al., 2007; Álvarez et al., 2023) with values up to $2600 \mu\text{mol kg}^{-1}$. The A_T and C_T
571 data obtained in 2014-2023 show a clear contrast between the northern and southern regions of the Western
572 Mediterranean Sea with higher concentration in the Ligurian Sea and the Gulf of Lion (Figure 7). This contrast is
573 associated to the circulation and the frontal system in this region (e.g. Barral et al, 2021). New data in the coastal
574 zones in the Gulf of Lion (ACCESS, DICASE, CARBODELTA, COCORICO2, MESURHOBENT) also have
575 very high A_T and C_T concentrations ($A_T > 2600 \mu\text{mol kg}^{-1}$; $C_T > 2350 \mu\text{mol kg}^{-1}$). Very low A_T and C_T
576 concentrations ($A_T < 2500 \mu\text{mol kg}^{-1}$; $C_T < 2200 \mu\text{mol kg}^{-1}$) were also occasionally observed in the coastal zones
577 (COCORICO2 stations, Petton et al, 2024).

578 In summer 2022 the Mediterranean Sea experienced an exceptional warming (Figure S6) superposed to
579 the long-term warming in the ocean (Cheng et al, 2024). Such event would impact the internal ocean processes
580 such as thermodynamic, stratification and biological processes (Coppola et al., 2023) and the inter-annual
581 variability and trends of C_T , pH, $f\text{CO}_2$ and air-sea CO_2 fluxes (Yao et al., 2016; Wimart-Rousseau et al., 2023;
582 Chau et al., 2024b). As in 2003, the warming in summer 2022 was associated to the drought event that occurred
583 in Europe and over the Mediterranean Sea (Faranda et al., 2023). In July 2022, the maximum temperature of
584 28.42°C was observed at station SOMLIT-Point-B. In the Ligurian Sea the temperature trend was faster in recent
585 years, $+0.173 \pm 0.072^\circ\text{C}$ per decade over 1990-2010 and $+0.678 \pm 0.143$ per decade over 2010-2023 (Figure
586 S6). With the new data added in the SNAPO-CO2-v2 synthesis (DYFAMED, MOOSE-ANTARES, and
587 MOOSE-GE) we evaluated a temperature trend of $+0.84 \pm 0.20^\circ\text{C}$ per decade over 1998-2022 indicating that
588 the discrete sampling captured the property changes at regional scale. Based on the data in the Ligurian Sea the
589 trends of C_T appeared faster in summer ($+1.53 \pm 0.46 \mu\text{mol kg}^{-1} \text{yr}^{-1}$) than in winter ($+0.94 \pm 0.64 \mu\text{mol kg}^{-1} \text{yr}^{-1}$,
590 Table 7). On the other hand, the trends of A_T were the same ($+0.72 \pm 0.36 \mu\text{mol kg}^{-1} \text{yr}^{-1}$ in winter and $+0.69 \pm$
591 $0.42 \mu\text{mol kg}^{-1} \text{yr}^{-1}$ in summer). The trend of C_T in surface in winter was close to the one derived at 100m (below
592 the Chl-a maximum), $C_T^{100\text{m}} = +1.10 \pm 0.17 \mu\text{mol kg}^{-1} \text{yr}^{-1}$ (Figure 8) whereas for A_T the trend was the same in
593 surface and at depth ($+0.76 \pm 0.12 \mu\text{mol kg}^{-1} \text{yr}^{-1}$). This suggests that the winter C_T data recorded the
594 anthropogenic CO_2 uptake of around $+1 \mu\text{mol kg}^{-1} \text{yr}^{-1}$, Figure S7). As noted by Touratier and Goyet (2009) the
595 C_T concentrations in the Mediterranean Sea should increase in parallel with the level of atmospheric
596 anthropogenic CO_2 . For an atmospheric CO_2 rate of $+2.16 \text{ppm yr}^{-1}$ over 1998-2023 (Lan et al., 2024) and at
597 fixed sea surface temperature (17.75°C), salinity (38.25) and A_T ($2567 \mu\text{mol kg}^{-1}$), the theoretical C_T increase
598 would be $+1.24 \mu\text{mol kg}^{-1} \text{yr}^{-1}$. Interestingly, an anthropogenic flux of $-0.3 \pm 0.02 \text{molC m}^{-2} \text{yr}^{-1}$ in the
599 Mediterranean Sea (Bourgeois et al., 2016) would correspond to an increase of C_T of $1.07 \pm 0.07 \mu\text{mol kg}^{-1} \text{yr}^{-1}$ in
600 the top 100 meters. This is again close to what is observed in winter or at 100m (Table 7, Figure 8). On the other
601 hand the faster C_T trend observed in surface waters during summer might be associated with a decrease in
602 biological production and/or changes in circulation/mixing over time that deserve specific investigations such as
603 analyzed for the oxygen budget in this region (Ulses et al, 2021). It is worth noting that the C_T and A_T trends in
604 coastal zones of the Mediterranean Sea are opposite to those observed offshore: for example at station



605 SOLEMIO (Bay of Marseille, Wimart-Rousseau et al., 2020) the C_T and A_T concentrations decreased over 2016-
606 2022 and thus opposed to the anthropogenic CO_2 signal, indicating that processes such as riverine inputs,
607 advection or biology control the carbonate system decadal variability at local scale. This calls for developing
608 dedicated complex biogeochemical models to resolve these processes (Barré et al., 2023, 2024), especially when
609 extreme events occurred, such as the very hot summer in 2024 with SST up to $30^\circ C$ in the Mediterranean Sea
610 (Platforms Buoy/Mooring AZUR, EOL and La Revellata, data available at <https://dataselection.coriolis.eu.org/>).
611 The data obtained in the Mediterranean Sea are important not only to validate biogeochemical models but also to
612 reconstruct the carbonate system from A_T and pCO_2 data (Chau et al., 2024a) as the global A_T /SSS relationships
613 (e.g. Carter et al., 2018) are not suitable for this region.

614

615

616

617

618

619

620

621

622

623

624

625

626

627

628

629

630

631

632

633

634

635

636

637

638

639

640

641

642

643

644

645

646

647

648

649

650

651

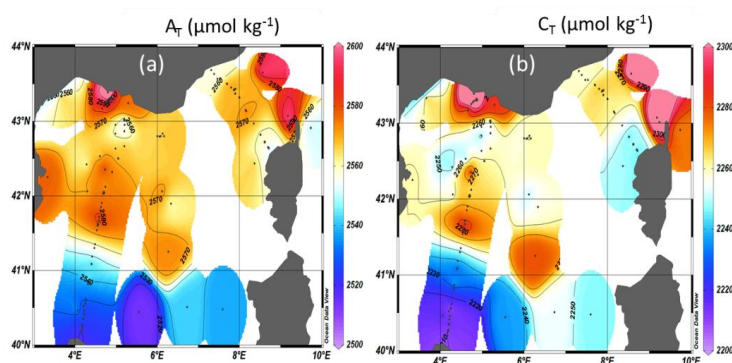


Figure 7: Distribution of A_T (a) and C_T (b) in $\mu mol kg^{-1}$ in surface waters of the Mediterranean Sea (0-10m) from observations over 2014-2023. Figures produced with ODV (Schlitzer, 2018).

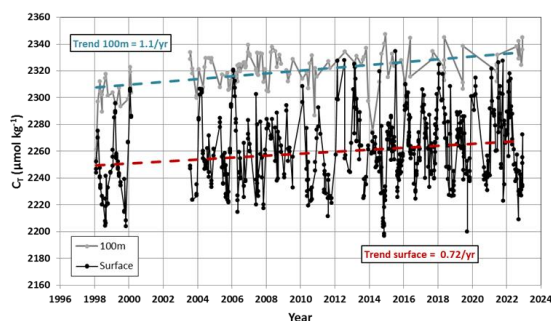


Figure 8: Time-series of C_T concentrations in surface (black symbols) and at 100m (grey symbols) in the Ligurian Sea. The trends over 1998-2022 is surface (red) and at 100m (blue) are indicated by dashed lines.

5.2 The North Atlantic

The North Atlantic Ocean is an important CO_2 sink (Takahashi et al. 2009) due to biological activity during summer, heat loss and deep convection during winter. As a result this region contains high concentrations of anthropogenic CO_2 (C_{ant}) in the water column (Khaliwala et al., 2013). Decadal variations of the C_{ant} inventories were recently identified at basin scale probably linked to the change of the overturning circulation



652 (Gruber et al., 2019; Müller et al., 2023; Pérez et al., 2024). This region experienced climate modes such as the
653 North Atlantic Oscillation (NAO) and the Atlantic Multidecadal Variability (AMV) that imprint variability in
654 air-sea CO₂ fluxes at inter-annual to multidecadal scales (e.g. Thomas et al., 2008; Jing et al., 2019;
655 Landschützer et al., 2019) but not always clearly revealed at regional scale (Metzl et al., 2010; Schuster et al.,
656 2013; Pérez et al., 2024). In addition it has been recently shown that extreme events such as the marine heat
657 wave in summer 2023 led to a reduce CO₂ uptake in this region (Chau et al., 2024b). Although the annual
658 CO₂ fluxes deduced from Global Ocean Biogeochemical Models (GOBM) seem coherent with the data-products
659 at basin scale (resp. -0.30 ± 0.07 and -0.24 ± 0.03 PgC/yr for the NA-SPSS biome) the $p\text{CO}_2$ cycle seasonality is
660 not well simulated (Pérez et al., 2024). Therefore to correct the GOBMs outputs, comparisons with the observed
661 C_T and A_T cycles are also needed.

662 In this context regular sampling in the North Atlantic (OVIDE cruises, Mercier et al., 2015, 2024;
663 SURATLANT transects, Reverdin et al., 2018) and time-series stations in the Irminger and Iceland Seas
664 (Ólafsson, et al., 2010; Lange et al., 2024; Yoder et al., 2024) are important to explore the variability of the
665 biogeochemical properties from seasonal (Figure S8) to decadal scales (Figure 9). The SURATLANT data added
666 in the SNAPO-CO2-v2 dataset over 2017-2023 offer new observations in the North Atlantic Subpolar Gyre
667 (NASPG in the NA-SPSS biome) and new transects from Norway to Iceland and reaching the coast of Greenland
668 (Figure 9). In 2010 the winter NAO was negative, moved to a positive state in 2012-2020 and was again very
669 low in 2021. The new SURATLANT data after 2017 confirm the cooling and the freshening in the NASPG since
670 2009 (Holliday et al., 2020; Leseurre et al., 2020; Siddiqui et al., 2024) whereas the most recent data in 2022 and
671 2023 suggest a reverse trend (increase of salinity and temperature, not shown). After 2016, large C_T anomalies in
672 the NASPG were observed. For examples, in April 2019 and 2022, the C_T concentrations were low compared to
673 2016 (Figure 9) and opposed to the expected anthropogenic CO₂ uptake. In September 2023 the C_T
674 concentrations were much lower than in 2022 (Figure 9) probably linked to biological productivity when the
675 NAO index was negative (Fröb et al., 2019) as observed in summer 2023 (NAO < -2 in July 2023). Despite these
676 variability the C_T trends are relatively well evaluated (Table 7). As in the Mediterranean Sea the C_T trends in the
677 NASPG appeared different depending on the season (Figure 9). The C_T increase was faster in September than in
678 April (resp. $+1.09 \pm 0.37 \mu\text{mol kg}^{-1} \text{yr}^{-1}$ and $+0.78 \pm 0.23 \mu\text{mol kg}^{-1} \text{yr}^{-1}$). This is either close to or lower than the
679 theoretical C_T increase due to the rising of atmospheric CO₂ ($+0.91 \mu\text{mol kg}^{-1} \text{yr}^{-1}$) and in the range of recent
680 results evaluated for the Sub-polar Mode Waters in the Irminger Sea (C_{ant} trend = $0.95 \pm 0.17 \mu\text{mol kg}^{-1} \text{yr}^{-1}$ for
681 the period 2009-2019, Curbelo-Hernández et al., 2024).

682

683

684

685

686

687

688

689

690

691

692

693

694

695

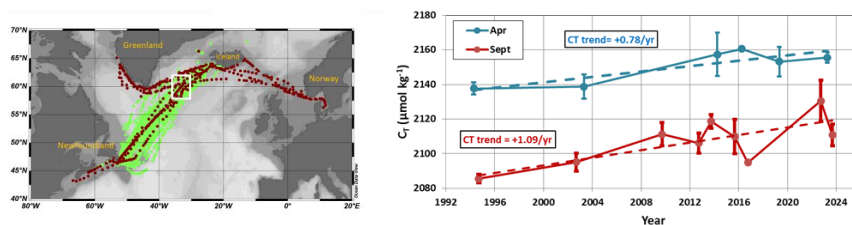


Figure 9: Left: Data in SNAPO-CO2-v1 (green) and new data in v2 (brown) from the SURATLANT cruises in 1993-2023 in the North Atlantic. Figure produced with ODV (Schlitzer, 2018). The white box identified the region of selected data around 60°N for the trend analysis. Right: Time-series of average C_T concentrations in April (blue) and September (red) in this region. The trends for each season are indicated (see also Table 7).



696

697 **5.3 The Tropical Atlantic**

698

699 In the Tropical Atlantic, previous studies highlighted the large variability of biogeochemistry and the
700 difficulty in detecting long-term trends of C_T (e.g. Lefèvre et al., 2021). This is related to the variability of
701 circulation, equatorial upwelling, biological processes (some linked to Saharan dust) and inputs from large rivers
702 (Congo, Amazon and Orinoco). The new data added in version SNAPO-CO2-v2 (Figure S9) show the
703 contrasting zonal C_T distribution in this region with lower concentrations in low salinity regions of the North
704 Equatorial Counter Current and Guinea Current (Figure 5; Oudot et al., 1995; Takahashi et al., 2014; Broullón et
705 al., 2020; Bonou et al., 2022). For exploring the temporal changes we selected the data in the western region
706 available for at least 10 years and separated the northern and southern sectors. In both regions the C_T trend is
707 close to $+3 \mu\text{mol kg}^{-1} \text{yr}^{-1}$ (Table 7, Figure S9) much higher than the expected anthropogenic signal. In this
708 region where coastal water masses mixes with oceanic waters, the inter-annual variability of C_T is large and the
709 changes driven by competitive processes (circulation, biological processes). More observations and dedicated
710 models are needed to separate the anthropogenic and natural variability in this region (Pérez et al., 2024).

711

712 **5.4 The Southern Ocean**

713

714 In the Southern Ocean there are a few regular multi-annual observations of the carbonate system. Time
715 series of more than 10 years were obtained in the Drake Passage (Munro et al., 2015) and in the Southern Indian
716 Ocean (Leseurre et al., 2022; Metzl et al., 2024b). Observations were also obtained for more than 20 years
717 southeast of New Zealand at the Munida Time Series (MTS) in the subtropical and sub-Antarctic frontal zones
718 (Currie et al., 2011; Vance et al., 2024). To complement these datasets we have added the data collected in the
719 South-Eastern Indian Ocean between Tasmania and Antarctica in the frame of the MINERVE cruises (Figure 10;
720 Brandon et al., 2022). These cruises were conducted from October to March offering each year a view of the
721 seasonal changes between late winter and summer from the sub-Antarctic zone to the coastal zone near
722 Antarctica (Adélie land). In all sectors (here from 45°S to 67°S) the C_T concentrations were higher in October
723 when the mixed-layer depth (MLD) was deep and were lower during the productive summer season (e.g. Laika
724 et al., 2009; Shadwick et al., 2015). An example is presented at $60^\circ\text{S}/151^\circ\text{E}$ from the data obtained along a
725 reoccupied track in 2011-2012 (Figure S10). At this location south of the Polar Front in the POOZ/HNLC area,
726 the C_T concentrations were $+25 \mu\text{mol kg}^{-1}$ higher in October compared to February. The same seasonal
727 amplitude was observed in the western Indian sector of the POOZ (Metzl et al., 2006, 2024b) suggesting that the
728 C_T seasonality is relatively homogeneous in this region corresponding to the Indian SO-SPSS biome (Fay and
729 McKinley, 2014). The difference in the climatological C_T between October and January is on average $+28.3 \pm$
730 $9.8 \mu\text{mol kg}^{-1}$ in the Indian Ocean POOZ (Takahashi et al., 2014). Given this seasonality and potential change in
731 the seasonal amplitude over time (Gallego et al., 2018; Landschützer et al., 2018; Shadwick et al., 2023) the
732 property trends have to be evaluated for October and January-February separately, here over 2002-2012 in the
733 POOZ (Figure 10, Table 7). In both seasons, the average C_T concentrations reached a minimum in 2008 and
734 increased faster in 2008-2012 (up to $+4.8 \mu\text{mol kg}^{-1} \text{yr}^{-1}$). Interestingly, such acceleration of the trend after 2009
735 was observed for $p\text{CO}_2$ at the MTS station (Vance et al., 2024). We note that the C_T trend over 2002-2012 was



736 slightly faster in October (Figure 10) probably linked to deeper MLD as suggested from the cooling and the
 737 salinity increase observed during this season (not shown).

738
 739

740

741

742

743

744

745

746

747

748

749

750

751

752

753

754

755

756

757

758

759

760

761

762

763

764

765

766

767

768

769

770

771

772

773

774

775

776

777

778

779

780

781

782

783

784

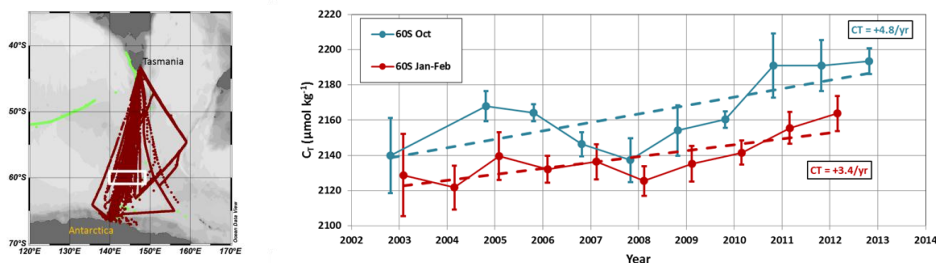


Figure 10: Left: Data in SNAPO-CO2-v1 dataset (green) and new data in version v2 (brown) in the South eastern Indian Ocean. Figure produced with ODV (Schlitzer, 2018). The white box identified the region of selected data around 60°S for the trend analysis. Right: Time-series of average C_T concentrations in January-February (red) and October (blue) around 60°S (white box in the map). The trends for each season are indicated (see also Table 7).

In the western Indian sector, the new data in the SNAPO-CO2-v2 dataset from the OISO cruises at high latitudes also recorded a rapid C_T trend over 5-8 years periods (e.g., $+3.4 \mu\text{mol kg}^{-1} \text{yr}^{-1}$ in 2015-2020 at 56°S, Figure 11, Table 7). Although the inter-annual variability of C_T , between 10 and 20 $\mu\text{mol kg}^{-1}$, is often recognized (Figure 11), the evaluation of the trends over more than 20 years indicated faster trend in the subtropical Indian Ocean ($+1.1 \mu\text{mol kg}^{-1} \text{yr}^{-1}$) compared to higher latitudes (Indian POOZ, $+0.6 \mu\text{mol kg}^{-1} \text{yr}^{-1}$); they are close to the expected anthropogenic signal in these regions ($+1.1 \mu\text{mol kg}^{-1} \text{yr}^{-1}$ in the subtropics and $+0.8 \mu\text{mol kg}^{-1} \text{yr}^{-1}$ at higher latitudes).

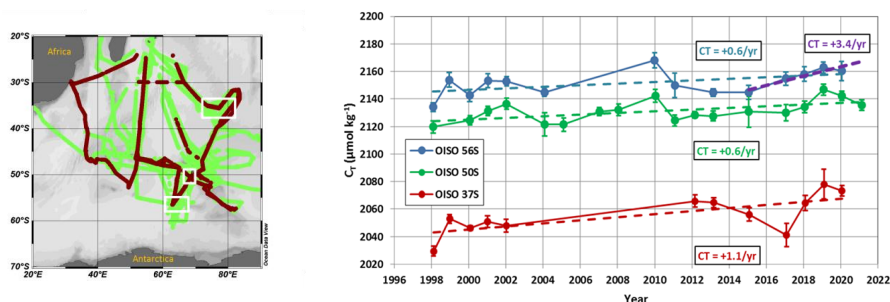


Figure 11: Left: Data in SNAPO-CO2-v1 dataset (green) and new data in version v2 (brown) in the South Western Indian Ocean (OISO cruises). Figure produced with ODV (Schlitzer, 2018). The white boxes identified the regions of data selected around 37°S, 50°S and 56°S for the trend analysis. Right: Time-series of average C_T concentrations in January-February at 37°S (red), 50°S (green) and 56°S (blue). The trends for each region are indicated (see also Table 7).



785 **Table 7:** Trend of C_T ($\mu\text{mol kg}^{-1} \text{ yr}^{-1}$) and corresponding standard error in selected regions where data are
 786 available for more than 10 years. The projects/cruises for selection of the data in each domain are indicated.
 787

788 Region	789 Period/Season	790 C_T trend ($\mu\text{mol kg}^{-1} \text{ yr}^{-1}$)	791 Projects/Cruises
792 North Atlantic (NASPG)	793 1994-2023 April	794 +0.78 (0.23)	795 SURATLANT
796 North Atlantic (NASPG)	797 1994-2023 September	798 +1.09 (0.37)	799 SURATLANT
800 West. Trop. Atl. 5N-Eq	801 2009-2021 April-October	802 +3.31 (2.13)	803 AMAZOMIX, PIRATA-BR, TARA
804 West. Trop. Atl. Eq-10S	805 2005-2015, April-October	806 +3.05 (1.64)	807 CAMFIN-WAT, PIRATA-BR, VOS
808 Ligurian Sea 8E	809 1998-2022 Jan-Feb.	810 +0.94 (0.64)	811 ANTARES, DYFAMED, MOOSE-GE
812 Ligurian Sea 8E	813 1998-2023 July-August	814 +1.53 (0.46)	815 ANTARES, DYFAMED, MOOSE-GE
816 Subtropical Indian 37S	817 1998-2020 Jan-Feb.	818 +1.12 (0.36)	819 OISO
820 South West. Indian 50S	821 1998-2021 Jan-Feb.	822 +0.61 (0.21)	823 OISO
824 South West. Indian 56S	825 1998-2020 Jan-Feb.	826 +0.58 (0.27)	827 OISO
828 South West. Indian 56S	829 2015-2020 Jan-Feb.	830 +3.41 (0.73)	831 OISO
832 South East. Indian 60S	833 2002-2012 Jan-Feb.	834 +3.37 (0.94)	835 MINERVE, OISO
836 South East. Indian 60S	2002-2012 October	+4.79 (1.62)	MINERVE

812 5.5 The Coastal Zones

813

814 Coastal waters experience enhanced ocean acidification due to increasing CO_2 uptake, accumulation of
 815 anthropogenic CO_2 (Bourgeois et al 2016; Laruelle et al, 2018; Roobaert et al, 2024a; Li et al, 2024) and from
 816 local anthropogenic inputs through rivers or from air pollution (e.g. Sarma et al, 2015; Sridvi and Sarma, 2021;
 817 Wimart-Rousseau et al, 2020). The changes of the CO_2 uptake in coastal zones are also linked to biological
 818 processes (Mathis et al, 2024) or to circulation and local upwelling (Roobaert et al, 2024b), all controlling large
 819 variability of A_T and C_T in space and time leading to uncertainties for detecting long-term changes of $p\text{CO}_2$ and
 820 air-sea CO_2 fluxes in heterogeneous coastal waters (Dai et al 2022; Resplandy et al, 2024). At seasonal scale,
 821 large differences between observations and models were also identified leading to differences in the coastal
 822 ocean CO_2 sink up to 60% (Resplandy et al, 2024). It is thus important to document the seasonal cycles of A_T and
 823 C_T to compare and correct models and thus to better predict future changes of biogeochemical properties in
 824 coastal waters and their impact on marine ecosystems. A better understanding of the processes and their
 825 retroaction in the coastal regions is also required regarding Marine Carbon Dioxide Removal (MCDR)
 826 experiments and for their evaluation (e.g. Ho et al, 2023).

827 In the SNAPO-CO2-v2 dataset new data have been added in the coastal zones at stations SOMLIT-
 828 Brest, SOMLIT-Roscoff and SOMLIT-Point-B. They extend the period to 2022 or 2023 for temporal analysis.
 829 New data in the French coastal zones have been also included from the COCORICO2 project documented in
 830 detail by Petton et al (2024). The observations in coastal zones could be identified in the MARCATS regions
 831 (Margins and CATCHment Segmentation, Laruelle et al, 2013) (Figure 12) where little information is available
 832 for quantifying the ocean CO_2 sink at the decadal scale and for evaluation of the anthropogenic CO_2 uptake
 833 (Regnier et al, 2013; Dai et al, 2022; Li et al, 2024). To explore the change of the observed properties in the
 834 coastal zones and have a flavor of the long-term C_T trends we selected the time series with at least 10 years of
 835 data (Table 8, Figure 13). Except at high latitudes (Greenland and Antarctic coastal zones), we observed a
 836 warming in coastal zones (not shown). Changes in salinity are also identified (increase or decrease) and results



837 of the trends are presented for salinity-normalized C_T at 34, 35 or 38 depending on the region. Although the
838 inter-annual variability is large in coastal waters, sometimes linked to extreme events (e.g. river discharges), we
839 observed an increase in $N-C_T$ at most of the 8 selected locations. The exceptions are the coastal zones in the Gulf
840 of Lion near the Rhone River and near Tasmania in October.

841 In the Gulf of Lion, the new data in the coastal zone confirmed the first view at the SOLEMIO station
842 over 2016-2018 (Bay of Marseille, Wimart-Rousseau et al, 2020). In this region the lowest C_T was observed in
843 summer 2022 (average C_T of $2238.6 \pm 21.0 \mu\text{mol kg}^{-1}$), much lower than in 2015 ($2290.8 \pm 44.7 \mu\text{mol kg}^{-1}$). Over
844 the continental shelf south of Tasmania (MARCATS #34), the trend in $N-C_T$ was positive in summer but not
845 significant in October. In October this was associated with an increase in Salinity and in A_T probably linked to
846 advective processes via the reversal and variability of the Zeehan or the East Australian currents. From our data a
847 warming of $+0.06^\circ\text{C yr}^{-1}$ was identified for both seasons over 2002-2012 as previously observed south of
848 Tasmania over 1991-2003 impacting the $p\text{CO}_2$ trend and air-sea CO_2 fluxes in this region (Borges et al, 2008).
849 The difference in the $N-C_T$ trends in austral summer and spring calls for new detail studies with extended data in
850 this region. At high latitude in the Adélie Land (Antarctic coast MARCATS #45), the variability of $N-C_T$ was
851 large (range from 2150 to 2200 $\mu\text{mol kg}^{-1}$, Figure 13) and the trend over 10 years in summer was not significant
852 (Table 8). As opposed to the open zone at 60°S (Figure 10) the C_T concentrations in the coastal zone near
853 Antarctica were not increasing, probably linked to competitive processes between anthropogenic uptake, changes
854 in primary production, mixing or ice melting (Shadwick et al, 2013, 2014). More data are needed to better
855 evaluate the changes of the carbonate system in Antarctic coastal zones where bottom waters are formed and
856 transport anthropogenic CO_2 at lower latitudes (Zhang et al, 2023).

857 For the coastal time series SOMLIT where annual trends could be estimated (sampling at monthly
858 resolution), the $N-C_T$ increase ($+2.1$ to $3.4 \mu\text{mol kg}^{-1} \text{yr}^{-1}$) is close or higher than the anthropogenic signal leading
859 to a decrease in pH ranging between -0.05 to -0.06 TS decade $^{-1}$. The new data added in the SNAPO- CO_2 -v2
860 dataset (2016-2023) confirm the progressive increase in C_T and the acidification in the western Mediterranean
861 Sea and in the North-East Atlantic coastal zones (Kapsenberg et al, 2017; Gac et al, 2021).

862
863
864
865
866
867
868
869
870
871
872
873
874
875
876
877
878

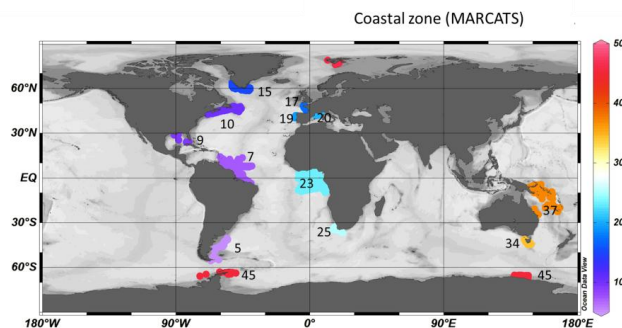


Figure 12: Location of $A_T C_T$ data available in the coastal zones in the SNAPO- CO_2 -v2 dataset. Numbers and Color code identify MARCATS region (Laruelle et al, 2013). Figure produced with ODV (Schlitzer, 2018).



879
 880
 881
 882
 883
 884
 885
 886
 887
 888
 889
 890
 891
 892
 893
 894
 895
 896
 897
 898
 899
 900
 901
 902
 903
 904
 905
 906
 907
 908
 909
 910
 911
 912
 913
 914
 915
 916
 917
 918
 919
 920
 921

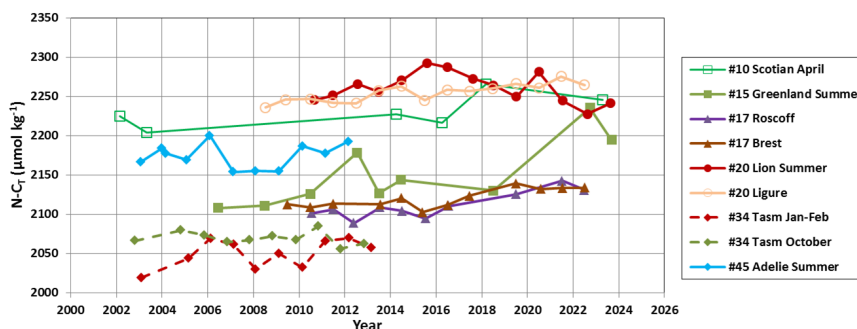


Figure 13: Time-series of average $N-C_T$ concentrations ($\mu\text{mol kg}^{-1}$) in selected MARCATS regions for different period when data are available for ten years or more. The trends and periods for each region are indicated in Table 8.

Table 8: Trends of $N-C_T$ ($\mu\text{mol kg}^{-1} \text{yr}^{-1}$) and corresponding standard errors in selected coastal regions where data are available for 10 years or more. The projects/cruises for selection of the data in each domain are indicated. MARCATS # regions also identified. Salinity value used for C_T normalization indicated.

Region #MARCATS	Period	Season	$N-C_T$ Trend ($\mu\text{mol kg}^{-1} \text{yr}^{-1}$)	Salinity	Projects/Cruises
Scotian #10	2002-2023	March-April	+1.71 (0.97)	35	SURATLANT
Greenland #15	2006-2023	June-mid-Sept	+5.77 (1.62)	35	OVIDE, SURATLANT
Roscoff #17	2010-2022	All season	+3.40 (0.76)	35	CHANNEL, COCORICO2, SOMLIT ROSCOFF
Bay of Brest #17	2009-2022	All seasons	+2.17 (0.52)	35	SOMLIT-Brest, COCORICO2, ECOSCOPA,
LION#20	2010-2023	June-Sept	-1.19 (1.25)	38	COCORICO2, MOOSE-GE, SOLEMIO (a)
LIGURE#20	2008-2022	All seasons	+2.12 (0.36)	38	SOMLIT-Point-B, MOOSE-GE
Tasmania #34	2003-2013	Jan-Feb	+2.73 (1.72)	35	MINERVE, OISO
Tasmania #34	2002-2012	Oct	-0.65 (0.89)	35	MINERVE, OISO
Adélie #45	2002-2012	Dec-Feb	+0.63 (0.70)	34	MINERVE, OISO

(a) For LION, some data in summer were also used from punctual cruises: AMOR-BFlux, CARBORHONE, DICASE, LATEX, MESURHOBENT, MISSRHODIA2 and MOLA.

6 Summary and suggestions

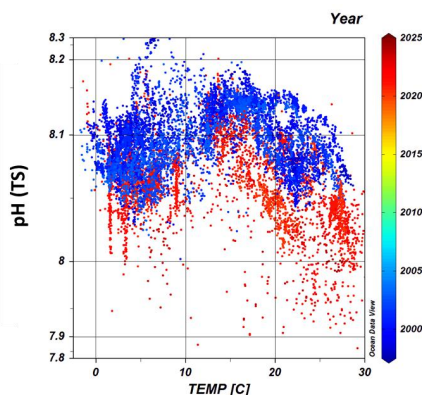
922
 923
 924
 925
 926
 927
 928
 929
 930
 931
 932
 933
 934

This work extends in time and new oceanic regions the A_T and C_T data presented in the first SNAPO-CO₂ synthesis (Metzl et al, 2024a). It includes now more than 67 000 surface and water column observations in all oceanic basins, in the Mediterranean Sea, in the coastal zones, near coral reefs, and in rivers. The data synthesized in version v2 are based on measurements of A_T and C_T performed between 1993 and 2023 with an accuracy of $\pm 4 \mu\text{mol kg}^{-1}$. Based on a secondary quality control, 91% of the A_T and C_T data are considered as good (WOCE Flag 2) and 6% probably good (Flag 3). For the open ocean this synthesis complements the SOCAT, GLODAP and SPOTS data products (Bakker et al., 2016; Lauvset et al., 2024; Lange et al, 2024). For the coastal sites this also complements the synthesis of coastal time-series in the Iberian Peninsula (Padin et al, 2020), in the Canadian Atlantic continental shelf (Gibb et al, 2023) and around North America (Fassbender et al., 2018; Jiang et al., 2021; Jiang et al 2024, in prep). The SNAPO-CO₂ dataset enables to investigate the seasonal cycles, the inter-annual variability and the decadal trends of A_T and C_T in various oceanic provinces. The same



935 temporal analyses could be investigated for other carbonate system properties such as $f\text{CO}_2$ or pH calculated
936 from A_T and C_T for air-sea CO_2 flux estimates or ocean acidification studies (Figure 14).

937
938
939
940
941
942
943
944
945
946
947
948
949
950
951
952



953 **Figure 14:** An example of observed ocean acidification derived from the SNAPO-CO₂-v2 dataset: pH (TS)
954 calculated with A_T and C_T data are presented as a function of temperature (°C) for years 1998-2002 (blue
955 symbols) and 2020-2023 (red symbols) and for salinity > 33 (Nb data selected with flag 2 = 11994). In recent
956 years the pH was lower. Figure produced with ODV (Schlitzer, 2018).
957

958 In almost all regions the new data in 2021-2023 indicated that the C_T concentrations were higher in
959 recent years. In regions where data are available for more than 2 decades, the time-series show an increase of sea
960 surface C_T (North Atlantic, Southern Indian Ocean and Ligurian Sea) with a rate close to or higher than the
961 changes expected from anthropogenic CO_2 uptake. It is also recognized that at seasonal scale the C_T trends could
962 be different. However, with the data in hand, the long-term trend of C_T cannot be quantified with confidence to
963 compare with the anthropogenic carbon uptake in some regions. This is the case in the eastern tropical Atlantic
964 subject to high inter-annual variability (Lefèvre et al., 2021, 2024) although new data have been added over
965 2005-2022 in this region (Table 1, Figure S9). When data are available for less than a decade the increase in C_T
966 was observed but the trend was uncertain due to large inter-annual variability (e.g. Adélie Land). An exception
967 was identified in the coastal zone in the Gulf of Lion (Mediterranean Sea) where summer data since 2010 present
968 a decrease in C_T most pronounced since 2015 (C_T trend = $-5.2 \pm 1.5 \mu\text{mol kg}^{-1} \text{yr}^{-1}$). Such C_T decrease over 10
969 years was also observed at the Hawaii Ocean Time series, HOT over 2010-2020 (Dore et al, 2009,
970 <https://hahana.soest.hawaii.edu/hot/hotco2/hotco2.html>, last access: 27 August 2024).

971 Although the A_T concentrations present significant inter-annual variability such as in the NASPG, in the
972 Topical Atlantic or the Adélie land and coastal zones, A_T appears relatively constant over time except at these
973 locations. In the open ocean, we observed an increase of A_T in the Southern Ocean south of the Polar Front
974 around 60°S in 2003-2012 not directly linked to salinity. In the coastal zones a decrease of A_T was pronounced
975 south of Greenland. In the coast in the Gulf of Lion, as observed for C_T , A_T decreased (A_T trend = $-2.8 \pm 1.2 \mu\text{mol}$
976 $\text{kg}^{-1} \text{yr}^{-1}$). This is opposed to the changes observed in the Ligurian Sea at station SOMLIT-Point-B, where C_T and
977 A_T increased over 2007-2015 (Kapsenberg et al, 2017) highlighting the contrasting C_T and A_T trends in the
978 Mediterranean coastal zones where ocean acidification is detected (here over 2008-2022, pH trend of -0.048
979 $\pm 0.003 \text{.decade}^{-1}$). With the continuous warming, reduced stratification and the rapid pH change observed in the
980 Mediterranean Sea, how the marine ecosystems will respond in the future should be addressed (e.g. Howes et al,



981 2015; Maugendre et al 2015; Lacoue-Labarthe et al, 2016). The SNAPO-CO2-v2 dataset could also be used to
982 explore and analyze the changes of the carbonate system occurring during extreme events such as marine heat
983 waves, rapid freshening, deep convection or high phytoplankton bloom events.

984 This dataset would also serve for validating autonomous platforms capable of measuring pH and $f\text{CO}_2$
985 properties (Sarmiento et al, 2023) and, along with other synthesis products (Jiang et al, 2024 in prep.), provides
986 an additional reference dataset for the development and validation of regional biogeochemical models for
987 simulating air-sea CO_2 fluxes. Thanks to the RECCAP2 stories, it has been recognized that Ocean
988 Biogeochemical Models present biases in the seasonal cycle of C_T and A_T due to inadequate representation of
989 biogeochemical cycles (e.g. Hauck et al, 2023; Rodgers et al, 2023; Sarma et al, 2023; Pérez et al, 2024;
990 Resplandy et al, 2024). The SNAPO-CO2-v2 dataset could be used to guide analyses for regional or global
991 biogeochemical models for A_T and C_T comparison and validation from seasonal to decadal scales. Our dataset is
992 also essential for training and validating neural networks capable of predicting variables in the carbonate system
993 (e.g. Fourier et al, 2020; Chau et al, 2024a; Gregor et al, 2024), thereby enhancing observations of marine CO_2 at
994 different spatial and temporal scales. Furthermore, we encourage the use of this dataset (or part of it), at sea or
995 prior going to sea for cruise planning. Indeed, using the approach of Davis and Goyet (2021) which takes into
996 account the multiple constraints (ship-time, number of samples, etc.), it is possible to determine the most
997 appropriate sampling strategy (Guglielmi et al., 2022, 2023), to reach the specific scientific objectives of each
998 cruise.

999 The data presented here are available online on the Seanoë server (<https://doi.org/10.17882/102337>) in a
1000 file identifying version v1 and v2. The sources of the original datasets (doi) with the associated references are
1001 listed in the Supplementary Material (Tables S3, S4). As for version v1 we invite the users to comment on any
1002 anomaly that would have not been detected or to suggest potential misqualification of data in the present product
1003 (e.g. data probably good although assigned with flag 3, probably wrong). As for SOCAT or GLODAP, we
1004 expect to update the SNAPO-CO2 dataset once new observations are obtained and controlled.

1005

1006 **7 Data availability**

1007 Data presented in this study are available at Seanoë (Metzl et al, 2024d, <https://www.seanoë.org>,
1008 <https://doi.org/10.17882/102337>. See also <https://doi.org/10.17882/95414> for version V1. The dataset is also
1009 available at <https://explore.webodv.awi.de/ocean/carbon/snapo-co2/>

1010

1011 *Author contributions.* NM prepared the data synthesis, the figures and wrote the draft of the manuscript with
1012 contributions from all authors. JF measured the discrete samples since 2014, with the help from CM and CLM,
1013 and prepared the individual reports for each project. NM and JF pre-qualified the discrete A_T/C_T data. CLM and
1014 NM are co-Is of the ongoing OISO project and qualified the underway A_T/C_T data from OISO cruises. FT and
1015 CG were PIs of the MINERVE cruises. All authors have contributed either to organizing cruises, sample
1016 collection and/or data qualification, and reviewed the manuscript.

1017

1018 *Competing interest.* The authors have the following competing interests: At least one of the (co-)authors is a
1019 member of the editorial board of Earth System Science Data

1020



1021 *Acknowledgments.* Most of the A_T and C_T data presented in this study were measured at the SNAPO-CO₂ facility
1022 (Service National d'Analyse des Paramètres Océaniques du CO₂) housed by the LOCEAN laboratory and part of
1023 the OSU ECCE Terra at Sorbonne University and INSU/CNRS analytical services. Support by INSU/CNRS, by
1024 OSU ECCE Terra and by LOCEAN, is gratefully acknowledged as well as support by different French "Services
1025 nationaux d'Observations", such as OISO/CARAUS, SOMLIT, PIRATA, SSS and MOOSE. We thank the
1026 research infrastructure ICOS (Integrated Carbon Observation System) France for funding a large part of the
1027 analyses. We thank the IRD (Institut de Recherche pour le Développement) and the French-Brazilian IRD-
1028 FAPEMA program for funding observations in the tropical Atlantic. We thank the French oceanographic fleet
1029 ("Flotte océanographique française") for financial and logistic support for most cruises listed in this synthesis
1030 and for the OISO program (<https://campagnes.flotteoceanographique.fr/series/228/>). We acknowledge the
1031 MOOSE program (Mediterranean Ocean Observing System for the Environment,
1032 <https://campagnes.flotteoceanographique.fr/series/235/fr/>) coordinated by CNRS-INSU and the Research
1033 Infrastructure ILICO (CNRS-IFREMER). The CocoriCO₂ project was founded by European Maritime and
1034 Fisheries Fund (grant no. 344, 2020–2023) and benefited from a subsidy from the Adour-Garonne water agency.
1035 We thank the following programs coordinated by A. Tribollet which have contributed to the acquisition of the
1036 data in Mayotte: CARBODISS funded by CNRS-INSU in 2018-2019, Future Maore reefs funded by Next
1037 Generation UE-France Relance in 2021-2023, and OA-ME funded by a Belmont Forum International (ANR) in
1038 2020-2026. We thank the program Mermex-Mistrals CNRS for supporting AMOR-BFlux, CARBORHONE,
1039 DICASE and MESURHOBENT cruises and the program EC2CO-INSU for supporting MISSRHODIA2 cruise.
1040 The ACCESS project was supported by CNRS MISTRALS and the DELTARHONE-1 by EC2CO-INSU. The
1041 ACIDHYPO project was founded by CNRS International Emerging Actions; we thank Captain and crew of the
1042 R/V Savannah from the Skidaway Institute of Oceanography (University of Georgia) for their support and
1043 technical assistance during the operations at sea. The AMAZOMIX project was funded by French
1044 Oceanographic Fleet, INSU (LEFE), IRD (LMI TAPICOA), CNES (TOSCA MIAMAZ project) and by the
1045 French-Brazilian international program GUYAMAZON. The OISO program was supported by the French
1046 institutes INSU (Institut National des Sciences de l'Univers) and IPEV (Institut Polaire Paul-Emile Victor), OSU
1047 Ecce-Terra (at Sorbonne Université), and the French program SOERE/Great-Gases. We also thank the Research
1048 Infrastructure ILICO (<https://www.ir-ilico.fr>). We warmly thank Alain Poisson who initiated the MINERVE
1049 program and performed many of the measurements onboard R/V Astrolabe from 2002 through 2018. We thank
1050 all colleagues and students who participated to the cruises and have carefully collected the precious seawater
1051 samples. We thank Frédéric Merceur (IFREMER) for preparing the page and data availability on Seanoe and
1052 Reiner Schlitzer (AWI) for including the SNAPO-CO₂ dataset in the ODV portal.

1053

1054

1055 **References:**

1056

1057 Ait Ballagh, F.E., Rabouille, C., Andrieux-Loyer, F. et al. Spatial Variability of Organic Matter and Phosphorus
1058 Cycling in Rhône River Prodelta Sediments (NW Mediterranean Sea, France): a Model-Data Approach.
1059 *Estuaries and Coasts* 44, 1765–1789, <https://doi.org/10.1007/s12237-020-00889-9>, 2021

1060

1061 Álvarez, M., Catalá, T. S., Civitarese, G., Coppola, L., Hassoun, A. E.R., Ibello, V., Lazzari, P., Lefevre, D.,
1062 Macías, D., Santinelli, C. and Ulses, C.: Chapter 11 - Mediterranean Sea general biogeochemistry, Editor(s):



- 1063 Katrin Schroeder, Jacopo Chiggiato, *Oceanography of the Mediterranean Sea*, Elsevier, Pages 387-451,
1064 <https://doi.org/10.1016/B978-0-12-823692-5.00004-2>, 2023.
1065
- 1066 Bakker, D. C. E., Pfeil, B., Landa, C. S., Metzl, N., O'Brien, K. M., Olsen, A., Smith, K., Cosca, C., Harasawa,
1067 S., Jones, S. D., Nakaoka, S.-I., Nojiri, Y., Schuster, U., Steinhoff, T., Sweeney, C., Takahashi, T., Tilbrook, B.,
1068 Wada, C., Wanninkhof, R., Alin, S. R., Balestrini, C. F., Barbero, L., Bates, N. R., Bianchi, A. A., Bonou, F.,
1069 Boutin, J., Bozec, Y., Burger, E. F., Cai, W.-J., Castle, R. D., Chen, L., Chierici, M., Currie, K., Evans, W.,
1070 Featherstone, C., Feely, R. A., Fransson, A., Goyet, C., Greenwood, N., Gregor, L., Hankin, S., Hardman-
1071 Mountford, N. J., Harlay, J., Hauck, J., Hoppema, M., Humphreys, M. P., Hunt, C. W., Huss, B., Ibáñez, J. S.
1072 P., Johannessen, T., Keeling, R., Kitidis, V., Körtzinger, A., Kozyr, A., Krasakopoulou, E., Kuwata, A.,
1073 Landschützer, P., Lauvset, S. K., Lefèvre, N., Lo Monaco, C., Manke, A., Mathis, J. T., Merlivat, L., Millero, F.
1074 J., Monteiro, P. M. S., Munro, D. R., Murata, A., Newberger, T., Omar, A. M., Ono, T., Paterson, K., Pearce, D.,
1075 Pierrot, D., Robbins, L. L., Saito, S., Salisbury, J., Schlitzer, R., Schneider, B., Schweitzer, R., Sieger, R.,
1076 Skjelvan, I., Sullivan, K. F., Sutherland, S. C., Sutton, A. J., Tadokoro, K., Telszewski, M., Tuma, M., Van
1077 Heuven, S. M. A. C., Vandemark, D., Ward, B., Watson, A. J., and Xu, S.: A multi-decade record of high-quality
1078 fCO₂ data in version 3 of the Surface Ocean CO₂ Atlas (SOCAT), *Earth Syst. Sci. Data*, 8, 383-413,
1079 doi:10.5194/essd-8-383-2016. 2016.
1080
- 1081 Barral, Q-B., Zakardjian, B. Dumas, F., Garreau, P., Testor, P., and Beuvier, J.: Characterization of fronts in the
1082 Western Mediterranean with a special focus on the North Balearic Front, *Progress in Oceanography*, Volume
1083 197, 102636, <https://doi.org/10.1016/j.pocean.2021.102636>. 2021
1084
- 1085 Barré, L., Diaz, F., Wagener, T., Van Wambeke, F., Mazoyer, C., Yohia, C., and Pinazo, C.: Implementation and
1086 assessment of a model including mixotrophs and the carbonate cycle (Eco3M_MIX-CarbOx v1.0) in a highly
1087 dynamic Mediterranean coastal environment (Bay of Marseille, France) – Part 1: Evolution of ecosystem
1088 composition under limited light and nutrient conditions, *Geosci. Model Dev.*, 16, 6701–6739,
1089 <https://doi.org/10.5194/gmd-16-6701-2023>, 2023.
1090
- 1091 Barré, L., Diaz, F., Wagener, T., Mazoyer, C., Yohia, C., and Pinazo, C.: Implementation and assessment of a
1092 model including mixotrophs and the carbonate cycle (Eco3M_MIX-CarbOx v1.0) in a highly dynamic
1093 Mediterranean coastal environment (Bay of Marseille, France) – Part 2: Towards a better representation of total
1094 alkalinity when modeling the carbonate system and air–sea CO₂ fluxes, *Geosci. Model Dev.*, 17, 5851–5882,
1095 <https://doi.org/10.5194/gmd-17-5851-2024>, 2024.
1096
- 1097 BERTRAND Arnaud, DE SAINT LEGER Emmanuel, KOCH-LARROUY Ariane : AMAZOMIX 2021 cruise,
1098 RV Antea, <https://doi.org/10.17600/18001364>, 2021
1099
- 1100 Bittig, H.C., Steinhoff, T., Claustre, H., Fiedler, B., Williams, N.L., Sauzède, R., Körtzinger, A. and Gattuso, J.-
1101 P.: An Alternative to Static Climatologies: Robust Estimation of Open Ocean CO₂ Variables and Nutrient
1102 Concentrations From T, S, and O₂ Data Using Bayesian Neural Networks. *Front. Mar. Sci.* 5:328. doi:
1103 10.3389/fmars.2018.00328, 2018
1104
- 1105 Bonou, F.K., Noriega, C., Lefèvre, N., Araujo, M.: Distribution of CO₂ parameters in the Western Tropical
1106 Atlantic Ocean, *Dynamics of Atmospheres and Oceans*, 73: 47-60
1107 <http://dx.doi.org/10.1016/j.dynatmoce.2015.12.001>, 2016
1108
- 1109 Bonou, F., Medeiros, C., Noriega, C., Araujo, M., Aubains Hounsou-Gbo, A., and Lefèvre N. : A comparative
1110 study of total alkalinity and total inorganic carbon near tropical Atlantic coastal regions. *J Coast Conserv* 26, 31,
1111 <https://doi.org/10.1007/s11852-022-00872-5>, 2022
1112
- 1113 Borges A.V., B. Tilbrook, N. Metzl, A. Lenton and B. Delille: Inter-annual variability of the carbon dioxide
1114 oceanic sink south of Tasmania, *Biogeosciences*, 5, 141-155. <https://doi.org/10.5194/bg-5-141-2008>, 2008
1115
- 1116 Bourgeois, T., J. C. Orr, L. Resplandy, J. Terhaar, C. Ethé, M. Gehlen, and L. Bopp: Coastal-ocean uptake of
1117 anthropogenic carbon. *Biogeosciences*, 13, 4167-4185, doi: 10.5194/bg-13-4167-2016., 2016
1118



- 1119 BOURLES Bernard (1997) PIRATA, <https://doi.org/10.18142/14>
1120
1121 BOURLES Bernard (2019) PIRATA FR29 cruise, RV Thalassa, <https://doi.org/10.17600/18000875>
1122
1123 BOURLES Bernard, LLIDO Jérôme (2020) PIRATA FR30 cruise, RV Thalassa,
1124 <https://doi.org/10.17600/18000690>
1125
1126 BOURLES Bernard, LLIDO Jérôme (2022) PIRATA FR32 cruise, RV Thalassa,
1127 <https://doi.org/10.17600/18001832>
1128
1129 Bozec Y., Cariou, T., Mace, E., Morin, P., Thuillier, D., Vernet, M.: Seasonal dynamics of air-sea CO₂ fluxes in
1130 the inner and outer Loire estuary (NW Europe). *Estuarine Coastal And Shelf Science*, 100, 58-71.
1131 <https://doi.org/10.1016/j.ecss.2011.05.015>, 2012
1132
1133 BOZEC Yann (2009) CO2ARVOR 3 cruise, RV Côtes De La Manche, <https://doi.org/10.17600/9480170>
1134
1135 BOZEC Yann (2009) CO2ARVOR 2 cruise, RV Côtes De La Manche, <https://doi.org/10.17600/9480110>
1136
1137 BOZEC Yann (2009) CO2ARVOR 1 cruise, RV Thalia, <https://doi.org/10.17600/9070070>
1138
1139 Brandon, M., C. Goyet, F. Touratier, N. Lefèvre, E. Kestenare, and R. Morrow : Spatial and temporal variability
1140 of the physical, carbonate and CO₂ properties in the Southern Ocean surface waters during austral summer
1141 (2005-2019). *Deep Sea Res. Part I*, 187, 103836, <https://doi.org/10.1016/j.dsr.2022.103836>, 2022
1142
1143 Broullón, D., Pérez, F. F., Velo, A., Hoppema, M., Olsen, A., Takahashi, T., Key, R. M., Tanhua, T., González-
1144 Dávila, M., Jeansson, E., Kozyr, A., and van Heuven, S. M. A. C.: A global monthly climatology of total
1145 alkalinity: a neural network approach, *Earth Syst. Sci. Data*, 11, 1109–1127, [https://doi.org/10.5194/essd-11-](https://doi.org/10.5194/essd-11-1109-2019)
1146 [1109-2019](https://doi.org/10.5194/essd-11-1109-2019), 2019
1147
1148 Broullón, D., Pérez, F. F., Velo, A., Hoppema, M., Olsen, A., Takahashi, T., Key, R. M., Tanhua, T., Santana-
1149 Casiano, J. M., and Kozyr, A.: A global monthly climatology of oceanic total dissolved inorganic carbon: a
1150 neural network approach, *Earth Syst. Sci. Data*, 12, 1725–1743, <https://doi.org/10.5194/essd-12-1725-2020>.
1151 2020
1152
1153 CARIOU Thierry, BOZEC Yann (2010) CO2ARVOR 4 cruise, RV Thalia, <https://doi.org/10.17600/10070040>
1154
1155 Carter, B. R., Feely, R. A., Williams, N. L., Dickson, A. G., Fong, M. B., and Takeshita, Y.: Updated methods
1156 for global locally interpolated estimation of alkalinity, pH, and nitrate. *Limnology and Oceanography: Methods*,
1157 16: 119-131. doi: 10.1002/lom3.10232, 2018
1158
1159 Chau, T.-T.-T., Gehlen, M., Metzl, N., and Chevallier, F.: CMEMS-LSCE: a global, 0.25°, monthly
1160 reconstruction of the surface ocean carbonate system, *Earth Syst. Sci. Data*, 16, 121–160,
1161 <https://doi.org/10.5194/essd-16-121-2024a>.
1162
1163 Chau, T.-T.-T., Chevallier, F., and Gehlen, M.: Global analysis of surface ocean CO₂ fugacity and air-sea fluxes
1164 with low latency. *Geophysical Research Letters*, 51, e2023GL106670. <https://doi.org/10.1029/2023GL106670>,
1165 2024b
1166
1167 Cheng, L. J., Abraham, J., Zhu, J., Trenberth, K. E., Fasullo, J., Boyer, T., Locarnini, R., Zhang, B., Yu, F. J.,
1168 Wan, L. Y., Chen, X. R., Song, X. Z., Liu, Y. L., and Mann, M. E.: Record-setting ocean warmth continued in
1169 2019, *Adv. Atmos. Sci*, 37, 137-142. <https://doi.org/10.1007/s00376-020-9283-7>, 2020
1170



- 1171 Cheng, L., Abraham, J., Trenberth, K.E. et al. New Record Ocean Temperatures and Related Climate Indicators
1172 in 2023. *Adv. Atmos. Sci.*, <https://doi.org/10.1007/s00376-024-3378-5>, 2024
1173
- 1174 Conan, P., Guieux, A., and Vuillemin, R.: MOOSE (MOLA), <https://doi.org/10.18142/234>, 2020.
1175
- 1176 Copin-Montégut, C.: Alkalinity and carbon budgets in the Mediterranean Sea, *Global Biogeochemical Cycles*,
1177 vol. 7, pp. 915–925, 1993.
1178
- 1179 Coppola, L., and Diamond-Riquier, E.: MOOSE (DYFAMED), <https://doi.org/10.18142/131>, 2008.
1180
- 1181 Coppola Laurent, Diamond Riquier Emilie, Carval Thierry, Irisson Jean-Olivier, Desnos Corinne: Dyfamed
1182 observatory data. SEANOE. <https://doi.org/10.17882/43749>, 2024
1183
- 1184 Coppola, L., Fourrier, M., Pasqueron de Fommervault, O., Poteau, A., Riquier, E. D. and Béguey, L.:
1185 Highresolution study of the air-sea CO₂ flux and net community oxygen production in the Ligurian Sea by a
1186 fleet of gliders. *Front. Mar. Sci.* 10:1233845. doi: 10.3389/fmars.2023.1233845, 2023
1187
- 1188 Curbelo-Hernández, D., Pérez, F. F., González-Dávila, M., Gladyshev, S. V., González, A. G., González-
1189 Santana, D., Velo, A., Sokov, A., and Santana-Casiano, J. M.: Ocean Acidification trends and Carbonate System
1190 dynamics in the North Atlantic Subpolar Gyre during 2009–2019, *EGUsphere* [preprint],
1191 <https://doi.org/10.5194/egusphere-2024-1388>, 2024.
1192
- 1193 Currie, K. I., Reid, M. R., and Hunter, K. A.: Interannual variability of carbon dioxide draw-down by
1194 subantarctic surface water near New Zealand, *Biogeochemistry*, 104, 23–34, <https://doi.org/10.1007/s10533-009-9355-3>, 2011.
1195
1196
- 1197 Cyronak, T., Santos, I. R., Erler, D. V., and Eyre, B. D.: Groundwater and porewater as major sources of
1198 alkalinity to a fringing coral reef lagoon (Muri Lagoon, Cook Islands), *Biogeosciences*, 10, 2467–2480,
1199 <https://doi.org/10.5194/bg-10-2467-2013>, 2013.
1200
- 1201 Dai, M., J. Su, Y. Zhao, E. E. Hofmann, Z. Cao, W. –J. Cai, J. Gan, F. Lacroix, G. G. Laruelle, F. Meng, J. D.
1202 Müller, P. A.G. Regnier, G. Wang, Z. Wang, 2022. Carbon Fluxes in the Coastal Ocean: Synthesis, Boundary
1203 Processes and Future Trends, *Annual Review of Earth and Planetary Sciences*, 50:1, 593–626,
1204 <https://doi.org/10.1146/annurev-earth-032320-090746>, 2022
1205
- 1206 Davis D. and Goyet, C.: *Balanced Error Sampling with applications to ocean biogeochemical sampling.*
1207 *Collection études*, Presses Universitaires de Perpignan, 224p. ISBN : 978-2-35412-452-6, 2021
1208
- 1209 Dickson, A. G., Sabine, C. L., and Christian, J. R.: *Guide to best practices for ocean CO₂ measurements*, North
1210 Pacific Marine Science Organization, Sidney, British Columbia, 191, <https://doi.org/10.25607/OBP-1342>, 2007.
1211
- 1212 DOE: *Handbook of Methods for Analysis of the Various Parameters of the Carbon Dioxide System in Seawater*;
1213 version 2, A.G. Dickson et C. Goyet, eds, ORNL/CDIAC-74, <https://doi.org/10.2172/10107773>, 1994.
1214
- 1215 Doney, S. C., Fabry, V. J., Feely, R. A., and Kleypas, J. A., Ocean acidification: The other CO₂ problem. *Annual*
1216 *Review of Marine Science*, 1(1), 169–192. [10.1146/annurev.marine.010908.163834](https://doi.org/10.1146/annurev.marine.010908.163834), 2009
1217
- 1218 Doney, S. C., Busch, D. S., Cooley, S. R., and Kroeker, K. J.: The Impacts of Ocean Acidification on Marine
1219 Ecosystems and Reliant Human Communities. *Annual Review of Environment and Resources* 45:1,
1220 <https://doi.org/10.1146/annurev-environ-012320-083019>. 2020
1221



- 1222 Dumoulin J-P, Pozzato L., Rassman J., Toussaint F., Fontugne M., Tisnerat-Laborde N., Beck L., Caffy I.,
1223 Delqué-Kolij E., Moreau C., Rabouille C. : Isotopic Signature (13C, 14C) of DIC in Sediment Pore Waters: An
1224 Example from the Rhone River Delta. *Radiocarbon*, 60(5), 1465-1481. <https://doi.org/10.1017/RDC.2018.111>,
1225 2018.
- 1226
1227 Dumoulin J-P, Rabouille C, Pourtout S, Bombled B, Lansard B, Caffy I, Hain S, Perron M, Sieudat M, Thellier
1228 B, Delqué-Kolij E, Moreau C, Beck L (2022). : Identification in Pore Waters of Recycled Sediment Organic
1229 Matter Using the Dual Isotopic Composition of Carbon (13C and 14C): New Data From the Continental Shelf
1230 Influenced by the Rhône River. *Radiocarbon*, 64(6), 1617-1627. <https://doi.org/10.1017/RDC.2022.71>, 2022.
- 1231
1232 Edmond, J. M.: High precision determination of titration alkalinity and total carbon dioxide content of sea water
1233 by potentiometric titration, *Deep-Sea Res.*, 17, 737–750, [https://doi.org/10.1016/0011-7471\(70\)90038-0](https://doi.org/10.1016/0011-7471(70)90038-0), 1970.
- 1234
1235 Eyring, V., Righi, M., Lauer, A., Evaldsson, M., Wenzel, S., Jones, C., Anav, A., Andrews, O., Cionni, I., Davin,
1236 E. L., Deser, C., Ehbrecht, C., Friedlingstein, P., Gleckler, P., Gottschaldt, K.-D., Hagemann, S., Juckes, M.,
1237 Kindermann, S., Krasting, J., Kunert, D., Levine, R., Loew, A., Mäkelä, J., Martin, G., Mason, E., Phillips, A. S.,
1238 Read, S., Rio, C., Roehrig, R., Senftleben, D., Sterl, A., van Ulft, L. H., Walton, J., Wang, S., and Williams, K.
1239 D.: ESMValTool (v1.0) – a community diagnostic and performance metrics tool for routine evaluation of Earth
1240 system models in CMIP, *Geosci. Model Dev.*, 9, 1747-1802, doi:10.5194/gmd-9-1747-2016, 2016.
- 1241
1242 Fabry, V. J., Seibel, B. A., Feely, R. A. and Orr, J. C.: Impacts of ocean acidification on marine fauna and
1243 ecosystem processes. *ICES J. Mar. Sci.* 65, 414–432. <https://doi.org/10.1093/icesjms/fsn048>, 2008.
- 1244
1245 Faranda, D., Pascale, S., Bulut, B.: Persistent anticyclonic conditions and climate change exacerbated the
1246 exceptional 2022 European-Mediterranean drought. *Environ. Res. Lett.*, 18, 034030, DOI 10.1088/1748-
1247 9326/abc37, 2023
- 1248
1249 Fassbender, A. J., Alin, S. R., Feely, R. A., Sutton, A. J., Newton, J. A., Krembs, C., Bos, J., Keyzers, M., Devol,
1250 A., Ruef, W., and Pelletier, G.: Seasonal carbonate chemistry variability in marine surface waters of the US
1251 Pacific Northwest, *Earth Syst. Sci. Data*, 10, 1367–1401, <https://doi.org/10.5194/essd-10-1367-2018>, 2018.
- 1252
1253 Fay, A. R., and McKinley, G. A.: Global open-ocean biomes: Mean and temporal variability. *Earth System*
1254 *Science Data*, 6(2), 273–284. <https://doi.org/10.5194/essd-6-273-2014>, 2014
- 1255
1256 Fourrier, M., Coppola, L., Claustre, H., D’Ortenzio, F., Sauzède, R. and Gattuso, J.-P.: A regional neural
1257 network approach to estimate water-column nutrient concentrations and carbonate system variables in the
1258 Mediterranean Sea: CANYON-MED. *Frontiers in Marine Science*, 7:620,
1259 <https://www.frontiersin.org/articles/10.3389/fmars.2020.00620>, 2020.
- 1260
1261 Friedlingstein, P., O’Sullivan, M., Jones, M. W., Andrew, R. M., Gregor, L., Hauck, J., Le Quéré, C., Luijkx, I.
1262 T., Olsen, A., Peters, G. P., Peters, W., Pongratz, J., Schwingshackl, C., Sitch, S., Canadell, J. G., Ciais, P.,
1263 Jackson, R. B., Alin, S. R., Alkama, R., Arnett, A., Arora, V. K., Bates, N. R., Becker, M., Bellouin, N., Bittig,
1264 H. C., Bopp, L., Chevallier, F., Chini, L. P., Cronin, M., Evans, W., Falk, S., Feely, R. A., Gasser, T., Gehlen,
1265 M., Gkritzalis, T., Gloege, L., Grassi, G., Gruber, N., Gürses, Ö., Harris, I., Hefner, M., Houghton, R. A., Hurtt,
1266 G. C., Iida, Y., Ilyina, T., Jain, A. K., Jersild, A., Kadono, K., Kato, E., Kennedy, D., Klein Goldewijk, K.,
1267 Knauer, J., Korsbakken, J. I., Landschützer, P., Lefèvre, N., Lindsay, K., Liu, J., Liu, Z., Marland, G., Mayot, N.,
1268 McGrath, M. J., Metzler, N., Monacci, N. M., Munro, D. R., Nakaoka, S.-I., Niwa, Y., O’Brien, K., Ono, T.,
1269 Palmer, P. I., Pan, N., Pierrot, D., Pockock, K., Poulter, B., Resplandy, L., Robertson, E., Rödenbeck, C.,
1270 Rodriguez, C., Rosan, T. M., Schwinger, J., Séférian, R., Shutler, J. D., Skjelvan, I., Steinhoff, T., Sun, Q.,
1271 Sutton, A. J., Sweeney, C., Takao, S., Tanhua, T., Tans, P. P., Tian, X., Tian, H., Tilbrook, B., Tsujino, H.,
1272 Tubiello, F., van der Werf, G. R., Walker, A. P., Wanninkhof, R., Whitehead, C., Willstrand Wranne, A.,
1273 Wright, R., Yuan, W., Yue, C., Yue, X., Zaehle, S., Zeng, J., and Zheng, B.: Global Carbon Budget 2022, *Earth*



- 1274 Syst. Sci. Data, 14, 4811–4900, <https://doi.org/10.5194/essd-14-4811-2022>, 2022.
- 1275
- 1276 Friedlingstein, P., O'Sullivan, M., Jones, M. W., Andrew, R. M., Bakker, D. C. E., Hauck, J., Landschützer, P.,
1277 Le Quéré, C., Luijkx, I. T., Peters, G. P., Peters, W., Pongratz, J., Schwingshackl, C., Sitch, S., Canadell, J. G.,
1278 Ciais, P., Jackson, R. B., Alin, S. R., Anthoni, P., Barbero, L., Bates, N. R., Becker, M., Bellouin, N., Decharme,
1279 B., Bopp, L., Brasika, I. B. M., Cadule, P., Chamberlain, M. A., Chandra, N., Chau, T.-T.-T., Chevallier, F.,
1280 Chini, L. P., Cronin, M., Dou, X., Enyo, K., Evans, W., Falk, S., Feely, R. A., Feng, L., Ford, D. J., Gasser, T.,
1281 Ghattas, J., Gkritzalis, T., Grassi, G., Gregor, L., Gruber, N., Gürses, Ö., Harris, I., Hefner, M., Heinke, J.,
1282 Houghton, R. A., Hurtt, G. C., Iida, Y., Ilyina, T., Jacobson, A. R., Jain, A., Jarníková, T., Jersild, A., Jiang, F.,
1283 Jin, Z., Joos, F., Kato, E., Keeling, R. F., Kennedy, D., Klein Goldewijk, K., Knauer, J., Korsbakken, J. I.,
1284 Körtzinger, A., Lan, X., Lefèvre, N., Li, H., Liu, J., Liu, Z., Ma, L., Marland, G., Mayot, N., McGuire, P. C.,
1285 McKinley, G. A., Meyer, G., Morgan, E. J., Munro, D. R., Nakaoka, S.-I., Niwa, Y., O'Brien, K. M., Olsen, A.,
1286 Omar, A. M., Ono, T., Paulsen, M., Pierrot, D., Pocock, K., Poulter, B., Powis, C. M., Rehder, G., Resplandy, L.,
1287 Robertson, E., Rödenbeck, C., Rosan, T. M., Schwinger, J., Séférian, R., Smallman, T. L., Smith, S. M.,
1288 Sospedra-Alfonso, R., Sun, Q., Sutton, A. J., Sweeney, C., Takao, S., Tans, P. P., Tian, H., Tilbrook, B., Tsujino,
1289 H., Tubiello, F., van der Werf, G. R., van Ooijen, E., Wanninkhof, R., Watanabe, M., Wimart-Rousseau, C.,
1290 Yang, D., Yang, X., Yuan, W., Yue, X., Zaehle, S., Zeng, J., and Zheng, B.: Global Carbon Budget 2023, Earth
1291 Syst. Sci. Data, 15, 5301–5369, <https://doi.org/10.5194/essd-15-5301-2023>, 2023.
- 1292
- 1293 Fröb, F., Olsen, A., Becker, M., Chafik, L., Johannessen, T., Reverdin, G., and Omar, A.: Wintertime fCO₂
1294 variability in the subpolar North Atlantic since 2004. *Geophysical Research Letters*, 46,
1295 <https://doi.org/10.1029/2018GL080554>, 2019.
- 1296
- 1297 Gac, J.-P., Marrec, P., Cariou, T., Grosstefan, E., Macé, E., Rimmelin-Maury, P., Vernet, M., and Bozec, Y.:
1298 Decadal Dynamics of the CO₂ System and Associated Ocean Acidification in Coastal Ecosystems of the North
1299 East Atlantic Ocean. *Front. Mar. Sci.* 8:688008. doi:10.3389/fmars.2021.688008, 2021.
- 1300
- 1301 Gallego, M. A., Timmermann, A., Friedrich, T., and Zeebe, R. E.: Drivers of future seasonal cycle changes in
1302 oceanic pCO₂, *Biogeosciences*, 15, 5315–5327, <https://doi.org/10.5194/bg-15-5315-2018>, 2018.
- 1303
- 1304 Gattuso, J.-P., Magnan, A., Billé, R., Cheung, W. W. L., Howes, E. L., Joos, F., Allemand, D., Bopp, L., Cooley,
1305 S., Eakin, M., Hoegh-Guldberg, O., Kelly, R. P., Pörtner, H.-O., Rogers, A. D., Baxter, J. M., Laffoley, D.,
1306 Osborn, D., Rankovic, A., Rochette, J., Sumaila, U. R., Treyer, S., and Turley, C.: Contrasting futures for ocean
1307 and society from different anthropogenic CO₂ emissions scenarios. *Science* 349:aac4722.doi:
1308 10.1126/science.aac4722, 2015.
- 1309
- 1310 Gattuso, Jean-Pierre; Alliouane, Samir; Mousseau, Laure (2021): Seawater carbonate chemistry in the Bay of
1311 Villefranche, Point B (France), January 2007 - June 2023 [dataset]. PANGAEA,
1312 <https://doi.org/10.1594/PANGAEA.727120>
- 1313
- 1314 Gibb, O., Cyr, F., Azetsu-Scott, K., Chassé, J., Childs, D., Gabriel, C.-E., Galbraith, P. S., Maillet, G., Pepin, P.,
1315 Punshon, S., and Starr, M.: Spatiotemporal variability in pH and carbonate parameters on the Canadian Atlantic
1316 continental shelf between 2014 and 2022, *Earth Syst. Sci. Data*, 15, 4127–4162, <https://doi.org/10.5194/essd-15-4127-2023>, 2023.
- 1317
- 1318
- 1319 Goyet, C., Beauverger, C., Brunet, C., and Poisson, A.: Distribution of carbon dioxide partial pressure in surface
1320 waters of the Southwest Indian Ocean, *Tellus B: Chemical and Physical Meteorology*, 43:1, 1-11, DOI:
1321 [10.3402/tellusb.v43i1.15242](https://doi.org/10.3402/tellusb.v43i1.15242), 1991.
- 1322
- 1323 Goyet C., Hassoun, A. E. R. Gemayel, E. Touratier, F., Abboud-Abi Saab M. and Guglielmi, V.:
1324 Thermodynamic forecasts of the Mediterranean Sea Acidification. *Mediterranean Marine Science*, 17/2, 508-
1325 518, <http://dx.doi.org/10.12681/mms.1487>, 2016
- 1326



- 1327 Goyet C., Benallal, M.A., Bijoux A., Guglielmi, V., Moussa, H., Ribou, A.-C., and Touratier, F.: Ch.39,
1328 Evolution of human Impact on Oceans: Tipping points of socio-ecological Coviability. In: Coviability of Social
1329 and Ecological Systems: Reconnecting Mankind to the Biosphere in an Era of Global Change. O.Barrière et al.
1330 (eds.) Springer International Publishing AG, part of Springer Nature 2019. [https://doi.org/10.1007/978-3-319-](https://doi.org/10.1007/978-3-319-78111-2_12)
1331 [78111-2_12](https://doi.org/10.1007/978-3-319-78111-2_12), 2019
1332
1333 Gregor, L. and Gruber, N.: OceanSODA-ETHZ: a global gridded data set of the surface ocean carbonate system
1334 for seasonal to decadal studies of ocean acidification, *Earth Syst. Sci. Data*, 13, 777–808,
1335 <https://doi.org/10.5194/essd-13-777-2021>, 2021.
1336
1337 Gregor, L., Shutler, J., and Gruber, N.: High-resolution variability of the ocean carbon sink. *Global*
1338 *Biogeochemical Cycles*, 38, e2024GB008127. <https://doi.org/10.1029/2024GB008127>, 2024
1339
1340 Gruber, N., Clement, D., Carter, B. R., Feely, R. A., van Heuven, S., Hoppema, M., Ishii, M., Key, R. M.,
1341 Kozyr, A., Lauvset, S. K., Lo Monaco, C., Mathis, J. T., Murata, A., Olsen, A., Perez, F. F., Sabine, C. L.,
1342 Tanhua, T., and Wanninkhof, R.: The oceanic sink for anthropogenic CO₂ from 1994 to 2007, *Science* vol. 363
1343 (issue 6432), pp. 1193-1199. DOI: 10.1126/science.aau5153, 2019.
1344
1345 Guglielmi V., Touratier, F., and Goyet, C.: Design of sampling strategy measurements of CO₂/carbonate
1346 properties. *Journal of Oceanography and Aquaculture*, DOI: 10.23880/ijoac-16000227, 2022
1347
1348 Guglielmi V., Touratier, F., and Goyet, C.: Determination of discrete sampling locations minimizing both the
1349 number of samples and the maximum interpolation error: Application to measurements of carbonate chemistry in
1350 surface ocean, *Journal of Sea Research*, <https://doi.org/10.1016/j.seares.2023.102336>, 2023
1351
1352 Hauck, J., Gregor, L., Nissen, C., Patara, L., Hague, M., Mongwe, P., et al.: The Southern Ocean carbon cycle
1353 1985–2018: Mean, seasonal cycle, trends, and storage. *Global Biogeochemical Cycles*, 37, e2023GB007848.
1354 <https://doi.org/10.1029/2023GB007848>, 2023
1355
1356 Ho, D. T., Bopp, L., Palter, J. B., Long, M. C., Boyd, P.W., Neukermans, G., and Bach, L. T.: Monitoring,
1357 reporting, and verification for ocean alkalinity enhancement. *State of the Planet*, 2-0ae2023, 1–12, 2023.
1358
1359 Holliday, N.P., Bersch, M., Berx, B., Chafik, L., Cunningham, S., Florindo-López, C., Hátún, H., Johns, W.,
1360 Josey, S.A., Larsen, K.M.H., Mulet, S., Oltmanns, M., Reverdin, G., Rossby, T., Thierry, V., Valdimarsson, H.,
1361 Yashayaev, I.: Ocean circulation causes the largest freshening event for 120 years in eastern subpolar North
1362 Atlantic. *Nat. Commun.*, 11. <https://doi.org/10.1038/s41467-020-14474-y>, 2020
1363
1364 Howes, E., Stemmann, L., Assailly, C., Irison, J.-O., Dima, M., Bijma, J., Gattuso, J.-P.: Pteropod time series
1365 from the North Western Mediterranean (1967-2003): impacts of pH and climate variability. *Mar Ecol Prog Ser*
1366 531: 193-206, doi: 10.3354/meps11322. 2015.
1367
1368 Huang, B., P. W. Thorne, V. F. Banzon, T. Boyer, G. Chepurin, J. H. Lawrimore, M. J. Menne, T. M. Smith, R.
1369 S. Vose, and H.-M. Zhang: Extended Reconstructed Sea Surface Temperature, version 5 (ERSSTv5): Upgrades,
1370 validations, and intercomparisons. *J. Climate*, 30, 8179-8205, doi:10.1175/JCLI-D-16-0836.1, 2017
1371
1372 IPCC. Changing Ocean, Marine Ecosystems, and Dependent Communities. in *The Ocean and Cryosphere in a*
1373 *Changing Climate* 447–588 (Cambridge University Press, 2022). doi:10.1017/9781009157964.007. 2022
1374
1375 Jiang, Z.-P., Tyrrell, T., Hydes, D. J., Dai, M., and Hartman, S. E.: Variability of alkalinity and the alkalinity-
1376 salinity relationship in the tropical and subtropical surface ocean, *Global Biogeochem. Cycles*, 28, 729–742,
1377 doi:10.1002/2013GB004678, 2014.
1378



- 1379 Jiang, L.-Q., Feely, R. A., Wanninkhof, R., Greeley, D., Barbero, L., Alin, S., Carter, B. R., Pierrot, D.,
1380 Featherstone, C., Hooper, J., Melrose, C., Monacci, N., Sharp, J. D., Shellito, S., Xu, Y.-Y., Kozyr, A., Byrne, R.
1381 H., Cai, W.-J., Cross, J., Johnson, G. C., Hales, B., Langdon, C., Mathis, J., Salisbury, J., and Townsend, D. W.:
1382 Coastal Ocean Data Analysis Product in North America (CODAP-NA) – an internally consistent data product for
1383 discrete inorganic carbon, oxygen, and nutrients on the North American ocean margins. *Earth System Science*
1384 *Data*, 13(6), 2777–2799. <https://doi.org/10.5194/essd-13-2777-2021>, 2021
1385
1386 Jiang, L.-Q., Dunne, J., Carter, B. R., Tjiputra, J. F., Terhaar, J., Sharp, J. D., et al.: Global surface ocean
1387 acidification indicators from 1750 to 2100. *Journal of Advances in Modeling Earth Systems*, 15,
1388 e2022MS003563. <https://doi.org/10.1029/2022MS003563>, 2023
1389
1390 Jiang, L.Q., Fay, A., Müller, J. D. et al: Synthesis products for ocean carbon chemistry. In prep., 2024.
1391 Jing, Y., Li, Y., Xu, Y., and Fan, G.: Influences of the NAO on the North Atlantic CO₂ fluxes in winter and
1392 summer on the interannual scale. *Advances in Atmospheric Sciences*, 36(11), 1288–1298.
1393 <https://doi.org/10.1007/s00376-019-8247-2>, 2019
1394
1395 Kapsenberg, L., Alliouane, S., Gazeau, F., Mousseau, L., and Gattuso, J.-P.: Coastal ocean acidification and
1396 increasing total alkalinity in the northwestern Mediterranean Sea, *Ocean Sci.*, 13, 411–426, doi:10.5194/os-13-
1397 411-2017, 2017.
1398
1399 Khatiwala, S., Tanhua, T., Mikaloff Fletcher, S., Gerber, M., Doney, S. C., Graven, H. D., Gruber, N.,
1400 McKinley, G. A., Murata, A., Ríos, A. F., and Sabine, C. L.: Global ocean storage of anthropogenic carbon,
1401 *Biogeosciences*, 10, 2169–2191, <https://doi.org/10.5194/bg-10-2169-2013>, 2013.
1402
1403 Koffi, U., Lefèvre, N., Kouadio, G., and Boutin, J.: Surface CO₂ parameters and air-sea CO₂ fluxes distribution
1404 in the eastern equatorial Atlantic Ocean. *J. Marine Systems*, doi:10.1016/j.jmarsys/2010.04.010. 2010.
1405
1406 Kwiatkowski, L., Torres, O., Bopp, L., Aumont, O., Chamberlain, M., Christian, J. R., Dunne, J. P., Gehlen, M.,
1407 Ilyina, T., John, J. G., Lenton, A., Li, H., Lovenduski, N. S., Orr, J. C., Palmieri, J., Santana-Falcón, Y.,
1408 Schwinger, J., Séférian, R., Stock, C. A., Tagliabue, A., Takano, Y., Tjiputra, J., Toyama, K., Tsujino, H.,
1409 Watanabe, M., Yamamoto, A., Yool, A., and Ziehn, T.: Twenty-first century ocean warming, acidification,
1410 deoxygenation, and upper-ocean nutrient and primary production decline from CMIP6 model projections,
1411 *Biogeosciences*, 17, 3439–3470, <https://doi.org/10.5194/bg-17-3439-2020>, 2020.
1412
1413 Lacoue-Labarthe, T., Nunes, P. A. L. D., Ziveri, P., Cinar, M., Gazeau, F., Hall-Spencer, J. M., Hilmi, N.,
1414 Moschella, P., Safa, A., Sauzade, D., and Turley, C.: Impacts of ocean acidification in a warming Mediterranean
1415 Sea: An overview, *Regional Studies in Marine Science*, 5, 1–11, doi:10.1016/j.rsma.2015.12.005, 2016.
1416
1417 Lagoutte, E., A. Tribollet, S. Bureau, et al., Biogeochemical evidence of flow re-entrainment on the main
1418 fringing reef of La Reunion Island, *Marine Chemistry*, <https://doi.org/10.1016/j.marchem.2024.104352>, 2023.
1419
1420 Laika, H. E., Goyet C., Vouve F., Poisson A., and Touratier F. : Interannual properties of the CO₂ system in the
1421 Southern Ocean south of Australia. *Antarctic Science*, 21(6), 663–680.
1422 <https://doi.org/10.1017/S0954102009990319>, 2009
1423
1424 Lan, X., Tans, P. and K.W. Thoning: Trends in globally-averaged CO₂ determined from NOAA Global
1425 Monitoring Laboratory measurements. Version 2024-08 <https://doi.org/10.15138/9NOH-ZH07> (last access: 14
1426 August 2024), 2024.
1427
1428 Landschützer, P., Gruber, N., Bakker, D. C. E., Stemmler, I., and Six, K. D.: Strengthening seasonal marine CO₂
1429 variations due to increasing atmospheric CO₂. *Nature Climate Change*, 8(2), 146–150.
1430 <https://doi.org/10.1038/s41558-017-0057-x>, 2018
1431



- 1432 Landschützer, P., Ilyina, T., and Lovenduski, N. S. : Detecting regional modes of variability in observation-
1433 based surface ocean pCO₂. *Geophysical Research Letters*, 46. <https://doi.org/10.1029/2018GL081756>, 2019
1434
- 1435 Lange, N., Fiedler, B., Álvarez, M., Benoit-Cattin, A., Benway, H., Buttigieg, P. L., Coppola, L., Currie, K.,
1436 Flecha, S., Gerlach, D. S., Honda, M., Huertas, I. E., Lauvset, S. K., Muller-Karger, F., Körtzinger, A., O'Brien,
1437 K. M., Ólafsdóttir, S. R., Pacheco, F. C., Rueda-Roa, D., Skjelvan, I., Wakita, M., White, A., and Tanhua, T.:
1438 Synthesis Product for Ocean Time Series (SPOTS) – a ship-based biogeochemical pilot, *Earth Syst. Sci. Data*,
1439 16, 1901–1931, <https://doi.org/10.5194/essd-16-1901-2024>, 2024.
1440
- 1441 LANSARD Bruno (2014) DICASE cruise, RV Téthys II, <https://doi.org/10.17600/14007100>
1442
- 1443 Laruelle, G. G., Dürr, H. H., Lauerwald, R., Hartmann, J., Slomp, C. P., Goossens, N., and Regnier, P. A. G.:
1444 Global multi-scale segmentation of continental and coastal waters from the watersheds to the continental
1445 margins, *Hydrol. Earth Syst. Sci.*, 17, 2029–2051, <https://doi.org/10.5194/hess-17-2029-2013>, 2013.
1446
- 1447 Laruelle, G. G. et al. Continental shelves as a variable but increasing global sink for atmospheric carbon dioxide.
1448 *Nat. Commun.* 9, 454, DOI: 10.1038/s41467-017-02738-z, 2018
1449
- 1450 Lauvset, S. K., Lange, N., Tanhua, T., Bittig, H. C., Olsen, A., Kozyr, A., Álvarez, M., Azetsu-Scott, K., Brown,
1451 P. J., Carter, B. R., Cotrim da Cunha, L., Hoppema, M., Humphreys, M. P., Ishii, M., Jeansson, E., Murata, A.,
1452 Müller, J. D., Pérez, F. F., Schirnick, C., Steinfeldt, R., Suzuki, T., Ulfsbo, A., Velo, A., Woosley, R. J., and
1453 Key, R. M.: The annual update GLODAPv2.2023: the global interior ocean biogeochemical data product, *Earth*
1454 *Syst. Sci. Data*, 16, 2047–2072, <https://doi.org/10.5194/essd-16-2047-2024>, 2024.
1455
- 1456 Lefèvre, D.: MOOSE (ANTARES), <https://doi.org/10.18142/233>, 2010.
1457
- 1458 Lefèvre N.: Carbon parameters along a zonal transect. SEANOE. <https://doi.org/10.17882/58575>, 2010.
1459
- 1460 Lefèvre Nathalie (2017). Carbon parameters in the gulf of Maranhao. SEANOE. <https://doi.org/10.17882/62417>
1461
- 1462 Lefèvre Nathalie (2018). Carbon parameters in the Western tropical Atlantic. SEANOE.
1463 <https://doi.org/10.17882/58406>
1464
- 1465 Lefèvre Nathalie (2019). Carbon parameters in the Eastern Tropical Atlantic in 2019. SEANOE.
1466 <https://doi.org/10.17882/83682>
1467
- 1468 Lefèvre Nathalie (2020). Inorganic carbon and alkalinity in the Eastern tropical Atlantic measured during the
1469 PIRATA FR-30 cruise in February-March 2020. SEANOE. <https://doi.org/10.17882/90742>
1470
- 1471 Lefèvre Nathalie (2022). Inorganic carbon and alkalinity in the Eastern tropical Atlantic in 2022. SEANOE.
1472 <https://doi.org/10.17882/92386>
1473
- 1474 Lefèvre, N., Urbano, D.F., Gallois, F., and Diverrès, D.: Impact of physical processes on the seasonal
1475 distribution of CO₂ in the western tropical Atlantic. *Journal of Geophysical Research* 119,
1476 doi: 10.1002/2013JC009248. doi: DOI: 10.1002/2013JC009248, 2014
1477
- 1478 Lefèvre, N., Veeda, D., Araujo, M., Caniaux, G.: Variability and trends of carbon parameters at a time series in
1479 the eastern tropical Atlantic. *Tellus B*, Co-Action Publishing, 68, pp.30305. 10.3402/tellusb.v68.30305. 2016.
1480
- 1481 Lefèvre N., da Silva Dias F. J., de Torres A. R., Noriega C., Araujo M., de Castro A. C. L., Rocha C., Jiang S.,
1482 Ibánhez J. S. P.: A source of CO₂ to the atmosphere throughout the year in the Maranhense continental shelf
1483 (2°30'S, Brazil). *Continental Shelf Research*, 141, 38-50. <https://doi.org/10.1016/j.csr.2017.05.004>, 2017a
1484



- 1485 Lefèvre N., Flores Montes M., Gaspar F. L., Rocha C., Jiang S., De Araújo M. C., Ibáñez J. S. P.: Net
1486 Heterotrophy in the Amazon Continental Shelf Changes Rapidly to a Sink of CO₂ in the Outer Amazon Plume.
1487 *Frontiers in Marine Science*, 4, -. <https://doi.org/10.3389/fmars.2017.00278>, 2017b
1488
1489 Lefèvre, N., Mejia, C., Khvorostyanov, D., Beaumont, L., and Koffi, U.: Ocean Circulation Drives the
1490 Variability of the Carbon System in the Eastern Tropical Atlantic. *Oceans*, 2021, 2, 126–148.
1491 <https://doi.org/10.3390/oceans2010008>, 2021.
1492
1493 Lefèvre, N., Veleda, D., Hartman, S.E.: Outgassing of CO₂ dominates in the coastal upwelling off the northwest
1494 African coast, Deep-Sea Research Part I, doi: <https://doi.org/10.1016/j.dsr.2023.104130>, 2023
1495
1496 Lefèvre, N., Veleda, D. and Beaumont, L.: Trends and drivers of CO₂ parameters, from 2006 to 2021, at a time-
1497 series station in the Eastern Tropical Atlantic (6°S, 10°W). *Front. Mar. Sci.* 11:1299071. doi:
1498 10.3389/fmars.2024.1299071, 2024
1499
1500 Leseurre, C.: Mécanismes de contrôle de l'absorption de CO₂ anthropique et de l'acidification des eaux dans les
1501 océans Atlantique Nord et Austral. PhD Thesis, Sorbonne Univ., 270 pp. <https://theses.hal.science/tel-04028410>,
1502 2022
1503
1504 Leseurre, C., Lo Monaco, C., Reverdin, G., Metzl, N., Fin, J., Olafsdottir, S., and Racapé, V.: Ocean carbonate
1505 system variability in the North Atlantic Subpolar surface water (1993–2017), *Biogeosciences*, 17, 2553–2577,
1506 <https://doi.org/10.5194/bg-17-2553-2020>, 2020
1507
1508 Leseurre, C., Lo Monaco, C., Reverdin, G., Metzl, N., Fin, J., Mignon, C., and Benito, L.: Summer trends and
1509 drivers of sea surface fCO₂ and pH changes observed in the southern Indian Ocean over the last two decades
1510 (1998–2019), *Biogeosciences*, 19, 2599–2625, <https://doi.org/10.5194/bg-19-2599-2022>, 2022.
1511
1512 Li, X., et al.: The source and accumulation of anthropogenic carbon in the U.S. East Coast, *Sci. Adv.* 10,
1513 eadl3169, DOI: 10.1126/sciadv.adl3169, 2024
1514
1515 LO MONACO Claire, METZL Nicolas (2019) VT 163 / OISO-29 cruise, RV Marion Dufresne,
1516 <https://doi.org/10.17600/18000972>
1517
1518 LO MONACO Claire (2020) OISO-30 cruise, RV Marion Dufresne, <https://doi.org/10.17600/18000679>
1519
1520 LO MONACO Claire, JEANDEL Catherine, PLANQUETTE Hélène (2021) OISO-31 cruise, RV Marion
1521 Dufresne, <https://doi.org/10.17600/18001254>
1522
1523 Lo Monaco, Claire; Metzl, Nicolas; Fin, Jonathan (2022). Sea surface measurements of dissolved inorganic
1524 carbon (DIC), total alkalinity (TALK), temperature and salinity during the R/V Marion-Dufresne Ocean Indien
1525 Service d'Observations - 29 (OISO-29) cruise (EXPOCODE 35MV20190106) in the Indian Ocean from 2019-
1526 01-06 to 2019-02-09 (NCEI Accession 0252612). NOAA National Centers for Environmental Information.
1527 Dataset. <https://doi.org/10.25921/8ajx-za24>. Accessed 14-Aug-2024.
1528
1529 Lo Monaco, Claire; Metzl, Nicolas (2023). Sea surface measurements of dissolved inorganic carbon (DIC), total
1530 alkalinity (TALK), temperature and salinity during the R/V Marion-Dufresne Ocean Indien Service
1531 d'Observations - 30 (OISO-30) cruise (EXPOCODE 35MV20200106) in the Indian Ocean from 2020-01-06 to
1532 2020-02-01 (NCEI Accession 0280937). NOAA National Centers for Environmental Information. Dataset.
1533 <https://doi.org/10.25921/n2g0-pp38>. Accessed 14-Aug-2024
1534
1535 Lo Monaco, Claire; Metzl, Nicolas; Fin, Jonathan (2023). Sea surface measurements of dissolved inorganic
1536 carbon (DIC), total alkalinity (TALK), temperature and salinity during the R/V Marion-Dufresne Ocean
1537 Indien Service d'Observations - 31 (OISO-31) cruise (EXPOCODE 35MV20210113) in the Indian Ocean



- 1538 from 2021-01-14 to 2021-03-04 (NCEI Accession 0280946). NOAA National Centers for Environmental
1539 Information. Dataset. <https://doi.org/10.25921/7sb2-k852>. Accessed 14-Aug-2024
- 1540
- 1541 Mathis, M., Lacroix, F., Hagemann, S. et al.: Enhanced CO₂ uptake of the coastal ocean is dominated by
1542 biological carbon fixation. *Nat. Clim. Chang.*, <https://doi.org/10.1038/s41558-024-01956-w>, 2024
- 1543
- 1544 Maugendre, L., J.-P. Gattuso, J. Louis, A. de Kluijver, S. Marro, K. Soetaert, F. Gazeau: Effect of ocean
1545 warming and acidification on a plankton community in the NW Mediterranean Sea, *ICES Journal of Marine*
1546 *Science*, Volume 72, Issue 6, July/August 2015, Pages 1744–1755, <https://doi.org/10.1093/icesjms/fsu161>, 2015
- 1547
- 1548 Mercier, H., Lherminier, P., Sarafanov, A., Gaillard, F., Daniault, N., Desbruyères, D., Falina, A., Ferron, B.,
1549 Huck, T., and Thierry, V.: Variability of the meridional overturning circulation at the Greenland-Portugal Ovide
1550 section from 1993 to 2010. *Progress in Oceanography*, 132, 250-261, [doi:10.1016/j.poccean.2013.11.001](https://doi.org/10.1016/j.poccean.2013.11.001). 2015
- 1551
- 1552 Mercier, H., Desbruyères, D., Lherminier, P., Velo, A., Carracedo, L., Fontela, M., and Pérez, F. F.: New
1553 insights into the eastern subpolar North Atlantic meridional overturning circulation from OVIDE, *Ocean Sci.*,
1554 20, 779–797, <https://doi.org/10.5194/os-20-779-2024>, 2024.
- 1555
- 1556 Metzl, N., Brunet, C., Jabaud-Jan, A., Poisson, A., and Schauer, B.: Summer and winter air-sea CO₂ fluxes in
1557 the Southern Ocean *Deep Sea Res I*, 53, 1548-1563, [doi:10.1016/j.dsr.2006.07.006](https://doi.org/10.1016/j.dsr.2006.07.006). 2006.
- 1558
- 1559 Metzl, N., Corbière, A., Reverdin, G., Lenton, A., Takahashi, T., Olsen, A., Johannessen, T., Pierrot, D.,
1560 Wanninkhof, R., Ólafsdóttir, S. R., Ólafsson, J., and Ramonet, M.: Recent acceleration of the sea surface fCO₂
1561 growth rate in the North Atlantic subpolar gyre (1993-2008) revealed by winter observations, *Global*
1562 *Biogeochem. Cycles*, 24, GB4004, [doi:10.1029/2009GB003658](https://doi.org/10.1029/2009GB003658), 2010.
- 1563
- 1564 Metzl, N., and Lo Monaco, C.: OISO - OCÉAN INDIEN SERVICE D'OBSERVATION,
1565 <https://doi.org/10.18142/228>, 1998.
- 1566
- 1567 Metzl, N., Lo Monaco, C., Leseurre, C., Ridame, C., Fin, J., Mignon, C., Gehlen, M., and Chau, T. T. T.: The
1568 impact of the South-East Madagascar Bloom on the oceanic CO₂ sink, *Biogeosciences*, 19, 1451–1468,
1569 <https://doi.org/10.5194/bg-19-1451-2022>, 2022
- 1570
- 1571 Metzl Nicolas, Fin Jonathan, Lo Monaco Claire, Mignon Claude, Alliouane Samir, Antoine David, Bourdin
1572 Guillaume, Boutin Jacqueline, Bozec Yann, Conan Pascal, Coppola Laurent, Douville Eric, Durrieu de Madron
1573 Xavier, Gattuso Jean-Pierre, Gazeau Frédéric, Golbol Melek, Lansard Bruno, Lefèvre Dominique, Lefèvre
1574 Nathalie, Lombard Fabien, Louanchi Férial, Merlivat Liliane, Olivier Léa, Petrenko Anne, Petton Sébastien,
1575 Pujo-Pay Mireille, Rabouille Christophe, Reverdin Gilles, Ridame Céline, Tribollet Aline, Vellucci Vincenzo,
1576 Wagener Thibaut, Wimart-Rousseau Cathy: SNAPO-CO₂ data-set: A synthesis of total alkalinity and total
1577 dissolved inorganic carbon observations in the global ocean (1993-2022). SEANOE.
1578 <https://doi.org/10.17882/95414>, 2023
- 1579
- 1580 Metzl, N., Fin, J., Lo Monaco, C., Mignon, C., Alliouane, S., Antoine, D., Bourdin, G., Boutin, J., Bozec, Y.,
1581 Conan, P., Coppola, L., Diaz, F., Douville, E., Durrieu de Madron, X., Gattuso, J.-P., Gazeau, F., Golbol, M.,
1582 Lansard, B., Lefèvre, D., Lefèvre, N., Lombard, F., Louanchi, F., Merlivat, L., Olivier, L., Petrenko, A., Petton,
1583 S., Pujo-Pay, M., Rabouille, C., Reverdin, G., Ridame, C., Tribollet, A., Vellucci, V., Wagener, T., and Wimart-
1584 Rousseau, C.: A synthesis of ocean total alkalinity and dissolved inorganic carbon measurements from 1993 to
1585 2022: the SNAPO-CO₂-v1 dataset, *Earth Syst. Sci. Data*, 16, 89–120, <https://doi.org/10.5194/essd-16-89-2024>,
1586 2024a
- 1587
- 1588 Metzl, N., Lo Monaco, C., Leseurre, C., Ridame, C., Reverdin, G., Chau, T. T. T., Chevallier, F., and Gehlen,
1589 M.: Anthropogenic CO₂, air-sea CO₂ fluxes, and acidification in the Southern Ocean: results from a time-series



- 1590 analysis at station OISO-KERFIX (51° S–68° E), *Ocean Sci.*, 20, 725–758, [https://doi.org/10.5194/os-20-725-](https://doi.org/10.5194/os-20-725-2024)
1591 2024, 2024b.
1592
1593 Metzl, N., C. Lo Monaco, G. Barut, and J.-F. Terner: Contrasting trends of the ocean CO₂ sink and pH in the
1594 Agulhas current system and the Mozambique Basin, South-Western Indian Ocean (1963–2023). *Sub DSRII*
1595 special issue IIOE-2, 2024c
1596
1597 Metzl Nicolas, Fin Jonathan, Lo Monaco Claire, Mignon Claude, Alliouane Samir, Bombled Bruno, Boutin
1598 Jacqueline, Bozec Yann, Comeau Steeve, Conan Pascal, Coppola Laurent, Cuet Pascale, Ferreira Eva, Gattuso
1599 Jean-Pierre, Gazeau Frédéric, Goyet Catherine, Grossteffan Emilie, Lansard Bruno, Lefèvre Dominique, Lefèvre
1600 Nathalie, Leseurre Coraline, Lombard Fabien, Petton Sébastien, Pujo-Pay Mireille, Rabouille Christophe,
1601 Reverdin Gilles, Ridame Céline, Rimmelin-Maury Peggy, Terner Jean-François, Touratier Franck, Tribollet
1602 Aline, Wagener Thibaut, Wimart-Rousseau Cathy (2024). An updated synthesis of ocean total alkalinity and
1603 dissolved inorganic carbon measurements from 1993 to 2023: the SNAPO-CO₂-v2 dataset. *SEANOE*.
1604 <https://doi.org/10.17882/102337>
1605
1606 MICHEL Elisabeth, VIVIER Frédéric (2016) STEP 2016 cruise, RV L'Atalante,
1607 <https://doi.org/10.17600/16000900>
1608
1609 Mu, L., Gomes, H. do R., Burns, S. M., Goes, J. I., Coles, V. J., Rezende, C. E., et al.: Temporal Variability of
1610 Air-Sea CO₂ flux in the Western Tropical North Atlantic Influenced by the Amazon River Plume. *Global*
1611 *Biogeochemical Cycles*, 35(6). <https://doi.org/10.1029/2020GB006798>, 2021
1612
1613 Munro, D. R., Lovenduski, N. S., Takahashi, T., Stephens, B. B., Newberger, T., and Sweeney, C.: Recent
1614 evidence for a strengthening CO₂ sink in the Southern Ocean from carbonate system measurements in the Drake
1615 Passage (2002–2015), *Geophys. Res. Lett.*, 42, 7623–7630, <https://doi.org/10.1002/2015GL065194>, 2015.
1616
1617 Müller, J. D., Gruber, N., Carter, B., Feely, R., Ishii, M., Lange, N., et al.: Decadal trends in the oceanic storage
1618 of anthropogenic carbon from 1994 to 2014. *AGU Advances*, 4, e2023AV000875.
1619 <https://doi.org/10.1029/2023AV000875>, 2023
1620
1621 Newton, J.A., Feely, R. A., Jewett, E. B., Williamson, P. and Mathis, J.: Global Ocean Acidification Observing
1622 Network: Requirements and Governance Plan. Second Edition, GOA-ON,
1623 <https://www.iaea.org/sites/default/files/18/06/goa-on-second-edition-2015.pdf>, 2015.
1624
1625 Olafsson, J., Olafsdottir, S. R., Benoit-Cattin, A., and Takahashi, T.: The Irminger Sea and the Iceland Sea time
1626 series measurements of sea water carbon and nutrient chemistry 1983–2008, *Earth Syst. Sci. Data*, 2, 99–104,
1627 <https://doi.org/10.5194/essd-2-99-2010>, 2010.
1628
1629 Olivier, L., Boutin, J., Reverdin, G., Lefèvre, N., Landschützer, P., Speich, S., Karstensen, J., Labaste, M.,
1630 Noisel, C., Ritschel, M., Steinhoff, T., and Wanninkhof, R.: Wintertime process study of the North Brazil
1631 Current rings reveals the region as a larger sink for CO₂ than expected, *Biogeosciences*, 19, 2969–2988,
1632 <https://doi.org/10.5194/bg-19-2969-2022>, 2022.
1633
1634 Olsen, A., Key, R. M., van Heuven, S., Lauvset, S. K., Velo, A., Lin, X., Schirnack, C., Kozyr, A., Tanhua, T.,
1635 Hoppema, M., Jutterström, S., Steinfeldt, R., Jeansson, E., Ishii, M., Pérez, F. F., and Suzuki, T.: The Global
1636 Ocean Data Analysis Project version 2 (GLODAPv2) – an internally consistent data product for the world ocean,
1637 *Earth Syst. Sci. Data*, 8, 297–323, <https://doi.org/10.5194/essd-8-297-2016>, 2016.
1638
1639 Oudot, C., Terner, J. F., and Lecomte, J.: Measurements of atmospheric and oceanic CO₂ in the tropical Atlantic:
1640 10 years after the 1982–1984 FOCAL cruises. *Tellus B: Chemical and Physical Meteorology*, 47(1–2), 70–85.
1641 <https://doi.org/10.3402/tellusb.v47i1-2.16032>, 1995
1642



- 1643 Padin, X. A., Velo, A., and Pérez, F. F.: ARIOS: a database for ocean acidification assessment in the Iberian
1644 upwelling system (1976–2018), *Earth Syst. Sci. Data*, 12, 2647–2663, [https://doi.org/10.5194/essd-12-2647-](https://doi.org/10.5194/essd-12-2647-2020)
1645 2020, 2020.
- 1646
- 1647 Palacio-Castro, A. M., Enochs, I. C., Besemer, N., Boyd, A., Jankulak, M., Kolodziej, G., et al.: Coral reef
1648 carbonate chemistry reveals interannual, seasonal, and spatial impacts on ocean acidification off Florida. *Global*
1649 *Biogeochemical Cycles*, 37, e2023GB007789. <https://doi.org/10.1029/2023GB007789>, 2023
- 1650
- 1651 Pardo, P. C., Tilbrook, B., Langlais, C., Trull, T. W., and Rintoul, S. R.: Carbon uptake and biogeochemical
1652 change in the Southern Ocean, south of Tasmania. *Biogeosciences*, 14(22), 5217–5237.
1653 <https://doi.org/10.5194/bg-14-5217-2017>, 2017.
- 1654
- 1655 Pérez, F. F., Becker, M., Goris, N., Gehlen, M., López-Mozos, M., Tjiputra, J., et al.: An assessment of CO₂
1656 storage and sea-air fluxes for the Atlantic Ocean and Mediterranean Sea between 1985 and 2018. *Global*
1657 *Biogeochemical Cycles*, 38, e2023GB007862. <https://doi.org/10.1029/2023GB007862>, 2024
- 1658
- 1659 Petton, S., Pernet, F., Le Roy, V., Huber, M., Martin, S., Macé, É., Bozec, Y., Loisel, S., Rimmelin Maury, P.,
1660 Grossteffan, É., Repecaud, M., Quemener, L., Retho, M., Manach, S., Papin, M., Pineau, P., Lacoue-Labarthe,
1661 T., Deborde, J., Costes, L., Polsenaere, P., Rigouin, L., Benhamou, J., Gouriou, L., Lequeux, J., Labourdette, N.,
1662 Savoye, N., Messiaen, G., Foucault, E., Ouisse, V., Richard, M., Lagarde, F., Voron, F., Kempf, V., Mas, S.,
1663 Giannecchini, L., Vidussi, F., Mostajir, B., Leredde, Y., Alliouane, S., Gattuso, J.-P., and Gazeau, F.: French
1664 coastal network for carbonate system monitoring: the CocoriCO₂ dataset, *Earth Syst. Sci. Data*, 16, 1667–1688,
1665 <https://doi.org/10.5194/essd-16-1667-2024>, 2024.
- 1666
- 1667 Petton Sébastien, Pernet Fabrice, Le Roy Valerian, Huber Matthias, Martin Sophie, Mace Eric, Bozec Yann,
1668 Loisel Stéphane, Rimmelin-Maury Peggy, Grossteffan Emilie, Repecaud Michel, Quéméner Loïc, Retho
1669 Michael, Manach Soazig, Papin Mathias, Pineau Philippe, Lacoue-Labarthe Thomas, Deborde Jonathan, Costes
1670 Louis, Polsenaere Pierre, Rigouin Loïc, Benhamou Jeremy, Gouriou Laure, Lequeux Joséphine, Labourdette
1671 Nathalie, Savoye Nicolas, Messiaen Gregory, Foucault Elodie, Lagarde Franck, Richard Marion, Ouisse
1672 Vincent, Voron Florian, Mas Sébastien, Giannecchini Léa, Vidussi Francesca, Mostajir Behzad, Leredde Yann,
1673 Kempf Valentin, Alliouane Samir, Gattuso Jean-Pierre, Gazeau Frédéric (2023). French coastal carbonate
1674 dataset from the CocoriCO₂ project. SEANOE. <https://doi.org/10.17882/96982>
- 1675
- 1676 Poisson, A., Culkin, F., and Ridout, P.: Intercomparison of CO₂ measurements. *Deep Sea Research Part A.*
1677 *Oceanographic Research Papers*, 37, 10, 1647-1650, [https://doi.org/10.1016/0198-0149\(90\)90067-6](https://doi.org/10.1016/0198-0149(90)90067-6), 1990.
- 1678
- 1679 Pozzato, L., Rassmann, J., Lansard, B., Dumoulin, J.-P., Van Breugel, P., and Rabouille, C.: Origin of
1680 remineralized organic matter in sediments from the Rhone River prodelta (NW Mediterranean) traced by Delta
1681 C-14 and delta C-13 signatures of pore water DIC. *Progress In Oceanography*, 163, 112-122.
1682 <https://doi.org/10.1016/j.poccean.2017.05.008>, 2018
- 1683
- 1684 RABOUILLE Christophe (2010) MESURHOBENT 1 cruise, RV Téthys II, <https://doi.org/10.17600/10450020>
- 1685
- 1686 RABOUILLE Christophe (2013) CARBODELTA cruise, RV Téthys II, <https://doi.org/10.17600/13450060>
- 1687
- 1688 RABOUILLE Christophe (2018) MISSRHODIA2 cruise, RV Téthys II, <https://doi.org/10.17600/18000473>
- 1689
- 1690 RABOUILLE Christophe, BOURRIN François, BASSETTI Maria-Angela (2022) DELTARHONE-1 cruise, RV
1691 Téthys II, <https://doi.org/10.17600/18002027>
- 1692
- 1693 Regnier, P., Friedlingstein, P., Ciais, P., Mackenzie, F. T., Gruber, N., et al: Anthropogenic perturbation of the
1694 carbon fluxes from land to ocean. *Nat. Geosci.* 6:597–607 , 2013.
- 1695



- 1696 Resplandy, L., Hogikyan, A., Müller, J. D., Najjar, R. G., Bange, H. W., Bianchi, D., et al.: A synthesis of global
1697 coastal ocean greenhouse gas fluxes. *Global Biogeochemical Cycles*, 38, e2023GB007803.
1698 <https://doi.org/10.1029/2023GB007803>, 2024
- 1699
- 1700 Revelle, R., and Suess, H. E.: Carbon dioxide exchange between atmosphere and ocean and the question of an
1701 increase of atmospheric CO₂ during the past decades. *Tellus* 9, 18–27. doi:10.1111/j.2153-
1702 3490.1957.tb01849.x, 1957.
- 1703
- 1704 Reverdin, G., Metzl, N., Olafsdottir, S., Racapé, V., Takahashi, T., Benetti, M., Valdimarsson, H., Benoit-Cattin,
1705 A., Danielsen, M., Fin, J., Naamar, A., Pierrot, D., Sullivan, K., Bringas, F., and Goni, G.: SURATLANT: a
1706 1993–2017 surface sampling in the central part of the North Atlantic subpolar gyre, *Earth Syst. Sci. Data*, 10,
1707 1901–1924, <https://doi.org/10.5194/essd-10-1901-2018>, 2018.
- 1708
- 1709 Reverdin, G., Metzl, N., Olafsdottir, S., Racapé, V., Takahashi, T., Benetti, M., Valdimarsson, H., Quay, P. D.,
1710 Benoit-Cattin, A., Danielsen, M., Fin, J., Naamar, A., Pierrot, D., Sullivan, K., Bringas, F., Goni, G., Becker M.,
1711 Leseurre C., and Olsen A.: SURATLANT: a surface dataset in the central part of the North Atlantic subpolar
1712 gyre. *SEANOE*. <https://doi.org/10.17882/54517>, 2023.
- 1713
- 1714 Rodgers, K. B., Schwinger, J., Fassbender, A. J., Landschützer, P., Yamaguchi, R., Frenzel, H., et al.: Seasonal
1715 variability of the surface ocean carbon cycle: A synthesis. *Global Biogeochemical Cycles*, 37, e2023GB007798.
1716 <https://doi.org/10.1029/2023GB007798>, 2023
- 1717
- 1718 Roobaert, A., Resplandy, L., Laruelle, G. G., Liao, E., and Regnier, P. : Unraveling the physical and biological
1719 controls of the global coastal CO₂ sink. *Global Biogeochemical Cycles*, 38, e2023GB007799.
1720 <https://doi.org/10.1029/2023GB007799>, 2024a
- 1721
- 1722 Roobaert, A., Regnier, P., Landschützer, P., and Laruelle, G. G.: A novel sea surface pCO₂-product for the
1723 global coastal ocean resolving trends over 1982–2020, *Earth Syst. Sci. Data*, 16, 421–441,
1724 <https://doi.org/10.5194/essd-16-421-2024>, 2024b.
- 1725
- 1726 Sarma, V. V. S. S., Krishna, M. S., Paul, Y. S., and Murty, V. S. N.: Observed changes in ocean acidity and
1727 carbon dioxide exchange in the coastal bay of Bengal—A link to air pollution. *Tellus B: Chemical and Physical*
1728 *Meteorology*, 67(1), 24638. <https://doi.org/10.3402/tellusb.v67.24638>, 2015
- 1729
- 1730 Sarma, V. V. S. S., Sridevi, B., Metzl, N., Patra, P. K., Lachkar, Z., Chakraborty, K., et al. : Air-sea fluxes of
1731 CO₂ in the Indian Ocean between 1985 and 2018: A synthesis based on observation-based surface CO₂, hindcast
1732 and atmospheric inversion models. *Global Biogeochemical Cycles*, 37, e2023GB007694.
1733 <https://doi.org/10.1029/2023GB007694>, 2023
- 1734
- 1735 Sarmiento, J.L., Johnson, K.S., Arteaga, L.A., Bushinsky, S.M., Cullen, H.M., Gray, A.R., Hotinski, R.M.,
1736 Maurer, T.L., Mazloff, M.R., Riser, S.C., Russell, J.L., Schofield, O.M., Talley, L.D., The Southern Ocean
1737 Carbon and Climate Observations and Modeling (SOCCOM) project: A review, *Progress in Oceanography*, doi:
1738 <https://doi.org/10.1016/j.pocean.2023.103130>, 2023
- 1739
- 1740 Schlitzer, R.: Ocean Data View, Ocean Data View, <http://odv.awi.de> (last access: 13 March 2019), 2018.
- 1741
- 1742 Schneider, A., Wallace, D. W. R., and Körtzinger, A.: Alkalinity of the Mediterranean Sea, *Geophys. Res. Lett.*,
1743 34, L15608, doi:10.1029/2006GL028842, 2007.
- 1744
- 1745 Schuster, U., McKinley, G. A., Bates, N., Chevallier, F., Doney, S. C., Fay, A. R., González-Dávila, M., Gruber,
1746 N., Jones, S., Krijnen, J., Landschützer, P., Lefèvre, N., Manizza, M., Mathis, J., Metzl, N., Olsen, A., Rios, A.
1747 F., Rödenbeck, C., Santana-Casiano, J. M., Takahashi, T., Wanninkhof, R., and Watson, A. J.: An assessment of



- 1748 the Atlantic and Arctic sea–air CO₂ fluxes, 1990–2009, *Biogeosciences*, 10, 607–627,
1749 <https://doi.org/10.5194/bg-10-607-2013>, 2013.
1750
- 1751 Shadwick, E., Rintoul, S., Tilbrook, B., Williams, G., Young, N., Fraser, A. D., et al.: Glacier tongue calving
1752 reduced dense water formation and enhanced carbon uptake. *Geophysical Research Letters*, 40(5), 904–909.
1753 <https://doi.org/10.1002/grl.50178>, 2013
1754
- 1755 Shadwick, E. H., B. Tilbrook, and G. D. Williams: Carbonate chemistry in the Mertz Polynya (East Antarctica):
1756 Biological and physical modification of dense water outflows and the export of anthropogenic CO₂, *J. Geophys.*
1757 *Res. Oceans*, 119, 1–14, doi:10.1002/2013JC009286, 2014
1758
- 1759 Shadwick, E. H., T. W. Trull, B. Tilbrook, A. J. Sutton, E. Schulz, and C. L. Sabine: Seasonality of biological
1760 and physical controls on surface ocean CO₂ from hourly observations at the Southern Ocean Time Series site
1761 south of Australia, *Global Biogeochem. Cycles*, 29, 223–238, doi:10.1002/2014GB004906, 2015
1762
- 1763 Shadwick, E. H., Wynn-Edwards, C. A., Matear, R. J., Jansen, P., Schulz, E. and Sutton, A. J.: Observed
1764 amplification of the seasonal CO₂ cycle at the Southern Ocean Time Series. *Front. Mar. Sci.* 10:1281854. doi:
1765 10.3389/fmars.2023.1281854, 2023
1766
- 1767 Siddiqui, A. H., Haine, T. W. N., Nguyen, A. T., and Buckley, M. W.: Controls on upper ocean salinity
1768 variability in the eastern subpolar North Atlantic during 1992–2017. *Journal of Geophysical*
1769 *Research: Oceans*, 129, e2024JC020887. <https://doi.org/10.1029/2024JC020887>, 2024
1770
- 1771 Sridevi, B., and Sarma, V. V. S. S.: Role of river discharge and warming on ocean acidification and pCO₂ levels
1772 in the Bay of Bengal. *Tellus B: Chemical and Physical Meteorology*, 73 (1), 1–20., DOI:
1773 10.1080/16000889.2021.1971924, 2021
1774
- 1775 Takahashi, T., Sutherland, S. C., Wanninkhof, R., Sweeney, C., Feely, R. A., Chipman, D. W., Hales, B.,
1776 Friederich, G., Chavez, F., Sabine, C., Watson, A. J., Bakker, D. C., Schuster, U., Metzl, N., Yoshikawa-Inoue,
1777 H., Ishii, M., Midorikawa, T., Nojiri, Y., Körtzinger, A., Steinhoff, T., Hoppema, M., Olafsson, J., Arnarson, T.
1778 S., Tilbrook, B., Johannessen, T., Olsen, A., Bellerby, R., Wong, C., Delille, B., Bates, N., and de Baar, H. J.:
1779 Climatological mean and decadal change in surface ocean pCO₂, and net sea air CO₂ flux over the global
1780 oceans. *Deep-Sea Res. II*, 56 (8–10), 554–577, <http://dx.doi.org/10.1016/j.dsr2.2008.12.009>. 2009.
1781
- 1782 Takahashi, T., Sutherland, S. C., Chipman, D. W., Goddard, J. G., Ho, C., Newberger, T., Sweeney, C. and
1783 Munro, D. R.: Climatological distributions of pH, pCO₂, total CO₂, alkalinity, and CaCO₃ saturation in the
1784 global surface ocean, and temporal changes at selected locations. *Marine Chemistry*, 164, 95–125,
1785 doi:10.1016/j.marchem.2014.06.004. 2014.
1786
- 1787 Ternon, J.-F., Oudot, C., Dessier, A., Diverres, D.: A seasonal tropical sink for atmospheric CO₂ in the Atlantic
1788 ocean: the role of the Amazon River discharge, *Marine Chemistry*, Volume 68, Issue 3, Pages 183–201,
1789 [https://doi.org/10.1016/S0304-4203\(99\)00077-8](https://doi.org/10.1016/S0304-4203(99)00077-8), 2000
1790
- 1791 TESTOR Pierre, COPPOLA Laurent, BOSSE Anthony (2021) MOOSE-GE 2021 cruise, RV Thalassa,
1792 <https://doi.org/10.17600/18001333>
1793
- 1794 TESTOR Pierre, COPPOLA Laurent, BOSSE Anthony (2022) MOOSE-GE 2022 cruise, RV Pourquoi pas ?,
1795 <https://doi.org/10.17600/18001854>
1796
- 1797 TESTOR Pierre, DURRIEU de MADRON Xavier (2023) MOOSE-GE 2023 cruise, RV Thalassa,
1798 <https://doi.org/10.17600/18002686>
1799



- 1800 Thomas, H., Prowe, A. E. F., Lima, I. D., Doney, S. C., Wanninkhof, R., Greatbatch, R. J., Schuster, U. and
1801 Corbière, A.: Changes in the North Atlantic Oscillation influence CO₂ uptake in the North Atlantic over the past
1802 2 decades, *Global Biogeochemical Cycles*, 22(4), doi:10.1029/2007GB003167, 2008
1803
1804 Tilbrook, B., Jewett, E. B., DeGrandpre, M. D., Hernandez-Ayon, J. M., Feely, R. A., Gledhill, D. K., Hansson,
1805 L., Isensee, K., Kurz, M. L., Newton, J. A., Siedlecki, S. A., Chai, F., Dupont, S., Graco, M., Calvo, E., Greeley,
1806 D., Kapsenberg, L., Lebrec, M., Pelejero, C., Schoo, K. L., and Telszewski, M.: An Enhanced Ocean
1807 Acidification Observing Network: From People to Technology to Data Synthesis and Information Exchange.
1808 *Frontiers in Marine Science*, 6, 337, DOI:10.3389/fmars.2019.00337, 2019.
1809
1810 TOURATIER Franck, POISSON Alain (1990) MINERVE, <https://doi.org/10.18142/128>
1811
1812 Touratier, F., and Goyet, C.: Decadal evolution of anthropogenic CO₂ in the north western Mediterranean Sea
1813 from the mid-1990's to the mid-2000's. *Deep Sea Research Part I*.doi:10.1016/j.dsr.2009.05.015, 2009.
1814
1815 Ulses, C., Estournel, C., Fourier, M., Coppola, L., Kessouri, F., Lefèvre, D., and Marsaleix, P.: Oxygen budget
1816 of the north-western Mediterranean deep- convection region, *Biogeosciences*, 18, 937–960,
1817 <https://doi.org/10.5194/bg-18-937-2021>, 2021.
1818
1819 Ulses, C., Estournel, C., Marsaleix, P., Soetaert, K., Fourier, M., Coppola, L., Lefèvre, D., Touratier, F., Goyet,
1820 C., Guglielmi, V., Kessouri, F., Testor, P., and Durrieu de Madron, X.: Seasonal dynamics and annual budget of
1821 dissolved inorganic carbon in the northwestern Mediterranean deep-convection region, *Biogeosciences*, 20,
1822 4683–4710, <https://doi.org/10.5194/bg-20-4683-2023>, 2023.
1823
1824 UNESCO: Intercomparison of total alkalinity and total inorganic carbon determinations in seawater. UNESCO
1825 Tech. Pap. Mar. Sci. 59., 1990
1826
1827 UNESCO: Reference materials for oceanic carbon dioxide measurements. UNESCO Tech. Pap. Mar. Sci. 60.,
1828 1991
1829
1830 United Nations. The Sustainable Development Goals 2020, 68pp. <https://unstats.un.org/sdgs/report/2020/>, 2020
1831
1832 Vance, J. M., Currie, K., Suanda, S. H. and Law, C. S.: Drivers of seasonal to decadal mixed layer carbon cycle
1833 variability in subantarctic water in the Munida Time Series. *Front. Mar. Sci.* 11:1309560. doi:
1834 10.3389/fmars.2024.1309560, 2024
1835
1836 VERNEY Romaric, RABOUILLE Christophe (2012) MERMEX-ACCESS cruise, RV Téthys II,
1837 <https://doi.org/10.17600/12450070>
1838
1839 VIVIER Frédéric, WAELBROECK Claire, MICHEL Elisabeth (2016) NEXT STEP,
1840 <https://doi.org/10.18142/338>
1841
1842 VERNEY Romaric, RABOUILLE Christophe (2012) MERMEX-ACCESS cruise, RV Téthys II,
1843 <https://doi.org/10.17600/12450070>
1844
1845 von Schuckmann, K., Minière, A., Gues, F., Cuesta-Valero, F. J., Kirchengast, G., Adusumilli, S., Straneo, F.,
1846 Ablain, M., Allan, R. P., Barker, P. M., Beltrami, H., Blazquez, A., Boyer, T., Cheng, L., Church, J.,
1847 Desbruyeres, D., Dolman, H., Domingues, C. M., García-García, A., Giglio, D., Gilson, J. E., Gorfer, M.,
1848 Haimberger, L., Hakuba, M. Z., Hendricks, S., Hosoda, S., Johnson, G. C., Killick, R., King, B., Kolodziejczyk,
1849 N., Korosov, A., Krinner, G., Kuusela, M., Landerer, F. W., Langer, M., Lavergne, T., Lawrence, I., Li, Y.,
1850 Lyman, J., Marti, F., Marzeion, B., Mayer, M., MacDougall, A. H., MacDougall, T., Monselesan, D. P., Nitzbon,
1851 J., Otosaka, I., Peng, J., Purkey, S., Roemmich, D., Sato, K., Sato, K., Savita, A., Schweiger, A., Shepherd, A.,
1852 Seneviratne, S. I., Simons, L., Slater, D. A., Slater, T., Steiner, A. K., Suga, T., Szekeley, T., Thiery, W.,



- 1853 Timmermans, M.-L., Vanderkelen, I., Wjiffels, S. E., Wu, T., and Zemp, M.: Heat stored in the Earth system
1854 1960–2020: where does the energy go?, *Earth Syst. Sci. Data*, 15, 1675–1709, [https://doi.org/10.5194/essd-15-](https://doi.org/10.5194/essd-15-1675-2023)
1855 1675-2023, 2023.
- 1856
- 1857 Wagener, T., Metz, N., Caffin, M., Fin, J., Helias Nunige, S., Lefevre, D., Lo Monaco, C., Rougier, G., and
1858 Moutin, T.: Carbonate system distribution, anthropogenic carbon and acidification in the western tropical South
1859 Pacific (OUTPACE 2015 transect), *Biogeosciences*, 15, 5221-5236, <https://doi.org/10.5194/bg-15-5221-2018>,
1860 2018.
- 1861
- 1862 Wimart-Rousseau, C.: Dynamiques saisonnière et pluriannuelle du système des carbonates dans les eaux de
1863 surface en mer Méditerranée, *Sciences de l'environnement*. Aix-Marseille Université, [https://hal.archives-](https://hal.archives-ouvertes.fr/tel-03523187)
1864 [ouvertes.fr/tel-03523187](https://hal.archives-ouvertes.fr/tel-03523187), 2021
- 1865
- 1866 Wimart-Rousseau, C., Lajaunie-Salla, K., Marrec, P., Wagener, T., Raimbault, P., Lagadec, V., Lafont, M.,
1867 Garcia, N., Diaz, F., Pinazo, C., Yohia, C., Garcia, F., Xueref-Remy, I., Blanc, P.-E., Armengaud, A., and
1868 Lefèvre, D.: Temporal variability of the carbonate system and air-sea CO₂ exchanges in a Mediterranean human-
1869 impacted coastal site. *Estuarine, Coastal and Shelf Science*. <https://doi.org/10.1016/j.ecss.2020.106641>, 2020.
- 1870
- 1871 Wimart-Rousseau, C., Wagener, T., Álvarez, M., Moutin, T., Fourier, M., Coppola, L., Niclas-Chirurgien, L.,
1872 Raimbault, P., D'Ortenzio, F., Durrieu de Madron, X., Taillandier, V., Dumas, F., Conan, P., Pujo-Pay, M. and
1873 Lefèvre, D.: Seasonal and Interannual Variability of the CO₂ System in the Eastern Mediterranean Sea: A Case
1874 Study in the North Western Levantine Basin. *Front. Mar. Sci.* 8:649246. doi: 10.3389/fmars.2021.649246, 2021
- 1875
- 1876 Wimart-Rousseau, C., Wagener, T., Bosse, A., Raimbault, P., Coppola, L., Fourier, M., Ulses, C. and Lefèvre,
1877 D.: Assessing seasonal and interannual changes in carbonate chemistry across two timeseries sites in the North
1878 Western Mediterranean Sea. *Front. Mar. Sci.* 10:1281003. doi: 10.3389/fmars.2023.1281003, 2023.
- 1879
- 1880 WMO/GCOS, 2018: <https://gcos.wmo.int/en/global-climate-indicators>, 2018
- 1881
- 1882 Yao, M. K., Marcou, O., Goyet, C., Guglielmi, V., Touratier, F., and Savy, J.-P.: Time variability of the north-
1883 western Mediterranean Sea pH over 1995-2011. *Marine Environmental Research*, doi:
1884 10.1016/j.marenvres.2016.02.016, 2016
- 1885
- 1886 Yoder, M. F., Palevsky, H. I., and Fogaren, K. E.: Net community production and inorganic carbon cycling in
1887 the central Irminger Sea. *Journal of Geophysical Research: Oceans*, 129, e2024JC021027.
1888 <https://doi.org/10.1029/2024JC021027>, 2024
- 1889
- 1890 Zhang, S., Wu, Y., Cai, W.-J., Cai, W., Feely, R. A., Wang, Z., et al. : Transport of anthropogenic carbon from
1891 the Antarctic shelf to deep Southern Ocean triggers acidification. *Global Biogeochemical Cycles*, 37,
1892 e2023GB007921. <https://doi.org/10.1029/2023GB007921>, 2023
- 1893